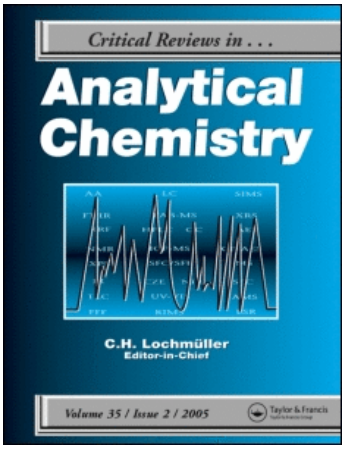

Critical Reviews in Analytical Chemistry
Publication details, including instructions for authors and subscription information:
http://www.informaworld.com/smpp/title~content=t713400837

Chronopotentiometry

Peter James Lingane; Dennis G. Peters

To cite this Article Lingane, Peter James and Peters, Dennis G.(1971) 'Chronopotentiometry', Critical Reviews in Analytical Chemistry, 1: 4, 587 — 634
To link to this Article: DOI: 10.1080/1040834nu08542742
URL: http://dx.doi.org/10.1080/1040834nu08542742

CHRONOPOTENTIOMETRY

Author: Peter James Lingane
Ledgemont Laboratory
Kennecott Copper Corp.
Lexington, Mass.

Referee: Dennis G. Peters
Department of Chemistry
Indiana University
Bloomington

TABLE OF CONTENTS

I. INTRODUCTION

By the term *chronopotentiometry* we mean an electrochemical technique in which a controlled current, usually a constant current, is caused to flow between two electrodes; the potential of one electrode is monitored as a function of time with respect to a suitable reference electrode. The solution is usually, but not necessarily, unstirred and contains an excess of a supporting electrolyte so that diffusion is the principal mechanism of mass transport. This technique is distinguished from *constant-current coulometric analysis* and *coulometric titrimetry*[1] in that the current in chronopotentiometry is sufficiently large that the current efficiency for the reduction of the species of interest falls below 100%, usually within a few seconds. It is distinguished from *galvanostatics*, a constant-current technique useful for the determination of heterogeneous electron-transfer rates,[2,3] in that the chronopotentiometric potential-time trace spans several hundred millivolts whereas the galvanostatic potential-time trace extends less than ten millivolts from the equilibrium potential.

This general area has been discussed previously[1, 5, 7-9, 14, 23] and I will attempt herein to complement rather than duplicate these reviews. No attempt has been made to make the literature review complete; numerous specific applications are discussed in Chapter XXII, reference 1; Table II, reference 7; and reference 23.

There are few, if any, *unique analytical applications* of chronopotentiometry.[5, 7] For example, the accuracy and scope of chronopotentiometry are very similar to that of classical polarography, yet the latter is 50 times more sensitive and better adapted to the analysis of mixtures.[6] Using solid electrodes, it is possible using chronopotentiometry to determine species which are oxidized only at potentials anodic to the dissolution potential of mercury. While it would be impossible to use classical polarography for such determinations, voltammetry with a rotating solid electrode would yield the same analytical information but with a greater sensitivity.

A promising area is chronopotentiometry in thin layers of solution. Since this area has been reviewed recently,[4] it will not be discussed here.

A typical chronopotentiometric trace is that for the oxidation of bis-(maleonitriledithiolate) platinum (II), $Pt(mnt)_2^{-2}$, in acetonitrile at a platinum electrode illustrated in Figure 1.[135] The

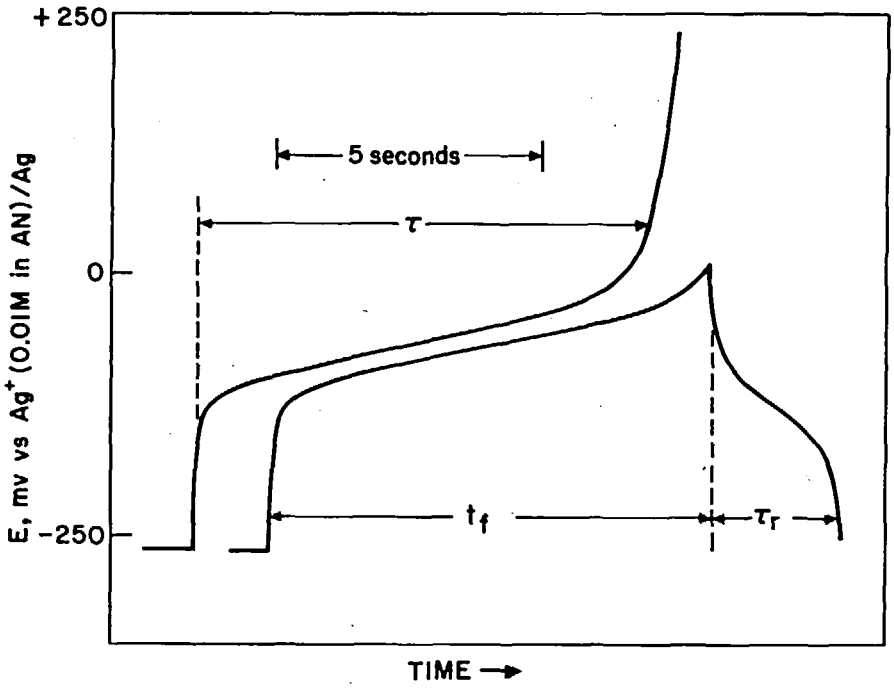

FIGURE 1. Chronopotentiogram for the oxidation of 1 m*M* $Pt(mnt)_2^{-2}$ in 0.1 *M* Et_4NClO_4 in acetonitrile at a platinum electrode. $i_o = 236\mu A/cm^2$.

qualitative potential-time behavior can be understood by noting that this system is reversible; that is, the potential of the working electrode is related to surface concentrations by the Nernst equation.

$$E = E^{\circ}_{Pt(mnt)_2^-,Pt(mnt)_2^{-2}} - 0.059 \log \frac{[Pt(mnt)_2^-]_{x=0}}{[Pt(mnt)_2^{-2}]_{x=0}}$$

Initially, the ratio of surface concentrations, designated here by the subscript $x = 0$, and hence the measured potential, changes rapidly as $Pt(mnt)_2^-$ is generated in a solution initially free of it. This is followed by a period in which the surface concentrations are about equal, so that their ratio is of the order of unity, and the potential changes more slowly. This potential region spans the standard potential of this couple, −0.10 V vs. Ag^+ (0.01 *M*)/ Ag. Since the constant current was chosen to be larger than the diffusion-limited value, the surface concentration of $Pt(mnt)_2^{-2}$ becomes very small after a few seconds and the ratio of surface concentrations changes more rapidly as the potential shifts to a value where a second electrode process can support part of the current. The time required to reach this potential shift, known as the *transition time* τ, is the fundamental measured quantity in chronopotentiometry.

Unlike controlled-potential techniques, the mass-transport boundary conditions in chronopotentiometry can be stated without introducing a relationship between electrode potential and surface concentrations. Since potential and surface concentrations are usually related via an exponential function, being able to avoid it in the boundary conditions makes the solution of chronopotentiometric problems less complex mathematically.

Perhaps this feature of chronopotentiometry can be shown most easily by comparing the derivation of the concentration profiles for both controlled-current and controlled-potential electrolyses. We will assume that we are dealing with the reduction $O + ne = R$ where both *O* and R are soluble in the solution and that the solution is initially free of R. The mass transport differential equations for which we seek solutions are

$$\frac{\partial C_O}{\partial t} = D_O \frac{\partial^2 C_O}{\partial x^2} \; ; \; \frac{\partial C_R}{\partial t} = D_R \frac{\partial^2 C_R}{\partial x^2} \qquad (1)$$

where we are specifically considering one-dimensional (i.e., semi-infinite linear) diffusion processes. C_O, D_O and C_R, D_R represent the concentration and diffusion coefficient of species O and R, respectively. The symbol t represents time and x, the distance coordinate.

The initial conditions and the three boundary conditions common to both chronopotentiometry and controlled-potential electrolyses are

$$C_O(x,0) = C^* \; ; \; C_R(x,0) = 0 \qquad (2)$$

$$D_O\left(\frac{\partial C_O}{\partial x}\right)_{x=0} + D_R\left(\frac{\partial C_R}{\partial x}\right)_{x=0} = 0 \qquad (3)$$

$$\lim_{x\to\infty} C_O(x,t) = C^* \qquad (4)$$

$$\lim_{x\to\infty} C_R(x,t) = 0 \qquad (5)$$

After transforming the differential equations into Laplace transform space,[10] we obtain for either controlled-potential or controlled-current conditions

$$\bar{C}_O(x,s) = \xi \exp[-\sqrt{sx^2/D_O}] - C^*/s \qquad (6)$$

$$\bar{C}_R(x,s) = \xi \exp[-\sqrt{sx^2/D_R}]$$

where the constant ξ remains to be evaluated from the fourth boundary condition.

For a controlled potential experiment, we have two choices. If the system is "reversible", the Nernst equation is the additional necessary boundary condition, i.e.,

$$C_O(0,t)/C_R(0,t) = \exp[\tfrac{nF}{RT}(E-E^{\circ\prime})] = \theta \qquad (7)$$

where $E^{\circ\prime}$ is the *formal* potential of the couple,

$$E^{\circ\prime} = E^{\circ} - \frac{RT}{nF} \ln \gamma_R/\gamma_O \qquad (8)$$

and where γ_R and γ_O are the activity coefficients of R and O and the resulting concentration profiles are functions of potential, distance from the electrode, and time.[11]

$$C_O(E,x,t) = C^*\left[\frac{D_O^{1/2}\theta + D_R^{1/2}\ \text{erf}\sqrt{x^2/4D_Ot}}{\theta D_O^{1/2} + D_R^{1/2}}\right] \quad (9)$$

$$C_R(E,x,t) = C^*\left[\frac{D_O^{1/2}\ \text{erf}\sqrt{x^2/4D_Rt}}{\theta D_O^{1/2} + D_R^{1/2}}\right] \quad (10)$$

The notations "erf" and "erfc" represent the error function and error function complement, (1–erf), respectively. The error function is equal to zero when its argument is zero and approaches unity when the argument is greater than about 2.

On the other hand, if the system is "irreversible," the appropriate boundary condition is [12]

$$i_o/nF = D_O\left(\frac{\partial C_O}{\partial x}\right)_{x=0} = k_fC_O(0,t) - k_bC_R(0,t) \quad (11)$$

where k_f and k_b are the heterogeneous electron-transfer rate constants appropriate to the reduction of O and the oxidation of R, respectively, and i_o is the current density. These rate constants are usually assumed to depend on potential in the following fashion.

$$k_f = k_{s,h}\exp\left[-\frac{\alpha nF}{RT}(E-E^o)\right] \quad (12)$$

$$k_b = k_{s,h}\exp\left[\frac{(1-\alpha)nF}{RT}(E-E^o)\right] \quad (13)$$

The quantity α is known as the transfer coefficient. The concentration profiles[13] appropriate to these boundary conditions are again functions of potential, distance, and time.

$$C_O(E,x,t) = \frac{C^*k_f}{QD_O^{1/2}}\left\{\text{erf}\sqrt{x^2/4D_Ot} + \exp\sqrt{Q^2x^2/D_O}\ \text{erfc}[Q\sqrt{t} + x^2/4D_Ot]\right\} \quad (14)$$

$$C_R(E,x,t) = C^* - \sqrt{D_O/D_R}\,C_O(E,x,t) \quad (15)$$

$$Q = k_f/D_O^{1/2} + k_b/D_R^{1/2} \quad (16)$$

On the other hand, only a single additional boundary condition is necessary to deduce the concentration profiles under chronopotentiometric conditions for *either* reversible or irreversible charge-transfer processes. Furthermore, this boundary condition does not involve the potential of the electrode.

$$i_o/nF = D_O\left(\frac{\partial C_O}{\partial x}\right)_{x=0} = F(t) \quad (17).$$

Most usually, F(t) is simply a constant. If the current is constant, the concentration profiles are

$$C_O(x,t) = C^* - \frac{2i_o}{nF}\sqrt{\frac{t}{\pi D_O}}\exp\left(\frac{-x^2}{4D_Ot}\right) + \frac{i_ox}{nFD_O}\ \text{erfc}\sqrt{x^2/4D_Ot} \quad (18)$$

$$C_R(x,t) = \frac{2i_o}{nF}\sqrt{\frac{t}{\pi D_R}}\exp\left(\frac{-x^2}{4D_Rt}\right) - \frac{i_ox}{nFD_R}\ \text{erfc}\sqrt{x^2/4D_Rt} \quad (19)$$

Note that these expressions, unlike the concentration profiles in a controlled-potential experiment, are independent of potential and of whether or not the electron-transfer process is reversible.

The measured quantity in chronopotentiometry, the *transition time* τ, is defined by $C_O(0,\tau) = 0$. With this definition, Equation 18 becomes

$$i_o\tau^{1/2}/C^* = nF\sqrt{\pi D_O}/2 = 85{,}520\ nD_O^{1/2} \quad (20)$$

This is known as the *Sand Equation.* It should be emphasized that Equations 18 to 20 are valid for both reversible and irreversible processes. The Sand Equation is equally valid if the *product* of the reaction is insoluble, or is adsorbed, or is destroyed in some chemical process (other than a catalytic one) following the electron-transfer step. We will see that the quantitative interpretation of the shape of the potential-time curve obtained will

depend on these factors but that the transition time does not.

One can draw an analogy with the polarographic current-potential curve. Although the shape of the wave and its position on the potential axis depend on the fate of the reaction products and on the kinetics of electron transfer, the limiting current does not.

In a sense, the argument just presented to demonstrate the relative mathematical simplicity of chronopotentiometry is unfair to controlled-potential techniques. For many applications, one controls the potential of the electrode such that C_O (0, t) is essentially zero; that is, for a cathodic process, at a value much more cathodic than the polarographic half-wave potential. Examples include analytical applications, the determination of adsorption,[15] and the elucidation of solution kinetics.[16] Under this circumstance, the mathematical superiority of chronopotentiometry disappears. Furthermore, in this age of the omnipresent computer, electroanalytical chemists have been very willing to solve mass transport problems by numerical methods including digital simulation where necessary[17,18] and, thus, the occasional mathematical superiority of chronopotentiometry is of diminishing importance.

To derive the shape of the chronopotentiometric potential-time curve, the surface concentrations of O and R, given by Equations 18 and 19 with x = 0, are introduced into Equation 11.

$$i_o/nF = k_f[C^* - \frac{2i_o}{nF}\sqrt{t/\pi D_O}] - k_b \frac{2i_o}{nF}\sqrt{t/\pi D_R} \qquad (21)$$

Introducing the potential dependence of k_f and k_b (Equations 12 and 13), evaluating C* in terms of the transition time calculated from the Sand Equation and rearranging, yields the following implicit relationship for the potential-time curve.

$$\frac{1}{k_{s,h}}\sqrt{\frac{\pi D_O}{4\tau}} - [1-\sqrt{\frac{t}{\tau}}]\exp[\frac{-\alpha nF}{RT}(E-E^{o'})] + \sqrt{\frac{tD_O}{\tau D_R}}\exp\left[\frac{(1-\alpha)nF}{RT}(E-E^{o'})\right]$$

$$= 0 \qquad (22)$$

(Another form of this expression appears later as Equation 75). There are two limiting situations. In the first, the lead term $\frac{1}{k_{s,h}}\sqrt{\frac{\pi D_O}{4\tau}}$ is so much smaller than the other terms that it can be neglected. This limit corresponds to fast kinetics (where $k_{s,h}$ is large) or long transition times. In this *reversible limit*, the equation for the potential-time curve becomes

$$E-E^{o'} = \frac{RT}{2nF}\ln D_R/D_O + \frac{RT}{nF}\ln[\sqrt{\tau/t}-1] \qquad (23)$$

Note the close analogy of the form of this equation to that for the polarographic potential-time curve for similar circumstances,[11] Equation 24.

$$E_{dme} - E^{o'} = \frac{RT}{2nF}\ln D_R/D_O + \frac{RT}{nF}\ln[i_d/i-1] \qquad (24)$$

For a reversible chronopotentiogram, the value of the potential at $t = \tau/4$ is equal to the polarographic half wave potential.

$$E_{1/4} = E^{o'} + \frac{RT}{2nF}\ln D_R/D_O = E_{1/2}$$

The polarographic notation ($E_{1/2}$) will be adopted in this review to avoid the introduction of unnecessary symbols. $E_{1/4}$ occurs very frequently in the chronopotentiometric literature, however.

The other limiting form for the equation of the chronopotentiometric potential-time curve is obtained when $\exp\left[\frac{(1-\alpha)nF}{RT}(E-E^{o'})\right]$ is very small so that the third term in the general expression can be neglected. This *totally irreversible limit* is equivalent to neglecting the second term in Equation 11; i.e., the rate of the back reaction R → O + ne is assumed to be negligible.

$$E - E^{o'} = \frac{RT}{\alpha nF}\ln\left[\sqrt{\frac{4\tau}{\pi D_O}}\,k_{s,h}\right] + \frac{RT}{nF}\ln[1-\sqrt{t/\tau}] \qquad (25)$$

This equation predicts that a plot of E vs. ln ($\tau^{1/2} - t^{1/2}$) or vs. ln $[1 - \sqrt{t/\tau}]$ will be linear with a slope proportional to $1/\alpha n$ and with an intercept at $t = 0$ which depends on the rate constant $k_{s,h}$. In this way one can, in principle, determine the parameters of the kinetics of the heterogeneous electron-transfer reaction by analyzing the shape of the potential-time curve, and its position on the potential axis, if the standard potential is known. This will be discussed further subsequently.

Finally, it should be pointed out that the potential-time curves we have been discussing are only a few of the many possibilities.[19] If the reduced form is formed at constant activity as in the deposition of a metal, or if one or both species are involved in homogeneous reactions, or if the reduction step produces monomeric species from dimeric ones or vice versa, then the particular relationships we have derived are not valid. But in all these cases the general approach is the same: determine $C_O(0, t)$ and $C_R(0, t)$ by solving the appropriate mass-transport equations and then introduce these expressions into Equation 11 or a more appropriate potential surface concentration relationship.

II. INSTRUMENTATION

An important advantage of chronopotentiometry in some circumstances is the rather simple instrumentation required. One circuit that is adequate for many purposes is illustrated in Figure 2. The constant-current source is constructed from a several-hundred-volt battery supply in series with a high-wattage variable resistance. Since the back emf of the cell plus the iR drop between the working and auxiliary electrodes is unlikely to exceed 2 or 3 volts, a 360 V battery supply will provide current regulation to better than 1%. Alternatively, a several-hundred-volt regulated-voltage power supply might be used.

S_1 serves as a current-reversing switch. S_2 is most simply a high-speed mercury-wetted relay (such as the C. P. Clare and Co. HGS-5000 series) which is used to switch the current from a dummy circuit to the cell circuit to start the experiment. Alternatively, solid state field effect transistor switching circuits[20] may be used. The current level is monitored as the iR drop across the precision resistor R_2 when S_2 is in the down position. Analogous designs[7] have required that the current measurement be made differentially; this is avoided here by grounding the working electrode. Since the working electrode is grounded, the output of the voltage follower is the potential of the reference electrode with respect to the working electrode; in other words, $-E$ where E is the potential of the working electrode with respect to the reference electrode. The dummy resistor R_3 is chosen such that the iR drop across

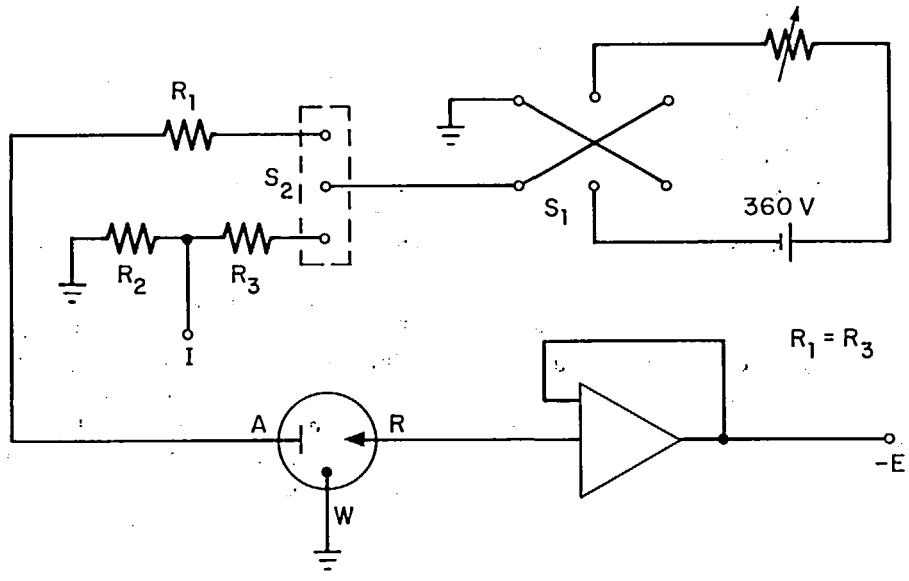

FIGURE 2. Simple battery-powered, constant-current source for chronopotentiometry. $R_1 = R_3 \sim 10^4$ ohms.

it approximates the iR drop across the cell; it can be left out for sufficiently large battery voltages.

There is one feature of this design which must be considered when one employs high current densities (short transition times) with large auxiliary electrodes and make-before-break relays at either S_1 or S_2.[21] Momentarily, for the millisecond period of the relay operation, the auxiliary and working electrodes are connected through some combination of R_1, R_2, and R_3. If these electrodes are at significantly different potentials, which will usually be the case unless the solution contains both members of the redox couple and the solution is stirred vigorously before the experiment, a potential spike is applied to the working electrode during the relay closure time. This spike may be minimized by using a small auxiliary electrode in the same solution and at least moderate values of R_1 and R_3 ($>10^4$ ohms).

Break-before-make switching devices have the disadvantage of permitting some recovery or change in the battery or supply voltage which may introduce a current spike when the circuit is closed again. A circuit has been devised which uses a fourth electrode to eliminate this problem.[22]

There are several types of constant current circuits based on operational amplifiers. One of the simplest, Figure 3A, operates by controlling the iR drop across R_L equal to $-e_{in}$. This has the effect of maintaining the current equal to $-e_{in}/R_L$. Note that the current will track e_{in} even if e_{in} is not constant so that this type of circuit is applicable for controlled-current experiments generally, as opposed to the more restricted constant-current capabilities of the circuit in Figure 2. This circuit has the disadvantage of requiring that the potential difference between the working and the reference electrodes be monitored with a differential follower amplifier. Of course, if one is operating at constant current and does not need to know the actual potential but only the change in potential with time (as in strictly analytical applications), a single-ended amplifier is satisfactory.

A second controlled-current circuit is shown in Figure 3B. Here the cell is placed directly in the feedback loop of the control amplifier. Disadvantages of this circuit are that a differential potential follower is again required and that the full cell current is drawn from the signal source.

A somewhat more elaborate set-up is shown in Figure 3C. This circuit operates by feeding back to the summing point on the control amplifier a signal proportional to the current. Here the working electrode is maintained at virtual ground by the current-measuring amplifier so that a single-ended potential follower amplifier is satisfactory. The greater complexity of this circuit is a disadvantage but this circuit can be converted to controlled-potential operation by switching S and this feature is the reason for this circuit's being incorporated into general-purpose electrochemical instruments.[24]

Apparatus for cyclic chronopotentiometry has been described.[25, 26]

III. THE MEASUREMENT OF ADSORPTION AND SURFACE FILM FORMATION

The major difficulty with chronopotentiometry arises in the interpretation of a measured transition time when several charge consuming processes operate in parallel. The difficulty with parallel charge-consuming processes arises because it is the current which is controlled in a chronopotentiometric experiment. Thus the *sum* of the rates of the parallel reactions is controlled while their relative rates are not. The data must be analyzed in terms of a mathematical model which at least approximates the manner in which the current is distributed among the several parallel reactions and, thus, any quantitative conclusions drawn from such data are model-dependent. One generally can only guess at the correct model; in fact, the elucidation of an appropriate model would usually dwarf the original problem in complexity.

During chronopotentiometric studies of electrode-surface "oxidation" and of the manner and the extent to which electrochemically active species are adsorbed onto the surfaces of electrodes, the current is distributed among at least three parallel processes:

a. faradaic reaction of adsorbed material or "oxide" film,

b. faradaic reaction of nonadsorbed diffusing material,

c. nonfaradaic charging of the electrode/electrolyte interface.

In this section we will focus our attention on the first two of these processes. Nonfaradaic double-layer charging will be dealt with subsequently.

In order to determine an adsorption isotherm, it is necessary to first develop an appropriate mechanism for the manner in which the current is

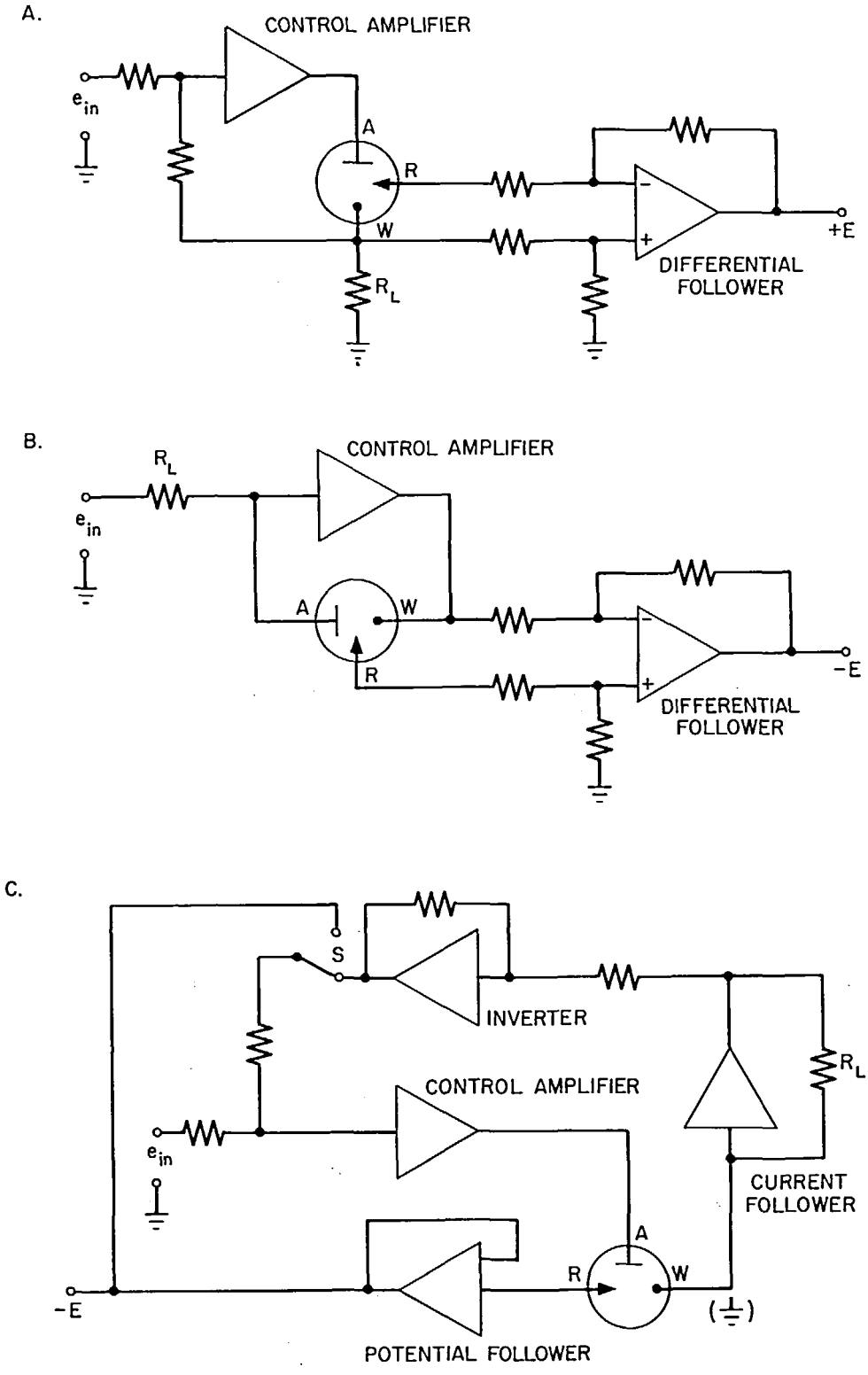

FIGURE 3. Controlled current sources for chronopotentiometry based on operational amplifiers. Except as noted, all resistors are 10^4 ohms. A. $i = -e_{in}/R_L$. B. $i = e_{in}/R_L$. C. $i = e_{in}/R_L$ when switch S is in the down position.

distributed among these processes. Unfortunately, a definitive *a priori* decision among the many possible models appears to be possible in only a minority of the cases.

By employing high current densities (and assuming that the effects of double-layer charging can be otherwise accounted for), the contribution due to the reaction of the diffusing material to the total charge will be minimized. Thus, for all adsorption models

$$\lim_{i_o \to \infty} i_o\tau = nF\Gamma \qquad (26)$$

where Γ is the surface density, in moles/cm,^{2} of the adsorbed material. This fact has been evoked by Rao et al.[27] in estimating the amount of "adsorbed oxygen" on a series of electrode surfaces. In general, it has not proven possible to obtain useful information in this fashion.

If the data are sufficiently precise, it should be possible to choose the model or models which best describe the data by testing for which of the possible models best "fit" the data. Two chronopotentiometric studies of specific systems[28, 29] have attempted to do just this by visually intercomparing various graphical treatments of the data; the authors of these studies have expressed reservations about the feasibility of their approach. It is difficult to draw any firm conclusions from these studies, however, since realistic models for the reaction of these adsorbed species are not known and were not determined and since neither the magnitude of the experimental error nor the manner in which the qualitative conclusions would be altered if more precise data were available was known.

Lingane[30] carried out an analysis of synthetic data in an attempt to gauge the extent to which the estimated values of the parameters depend upon the model according to which they were calculated. The use of synthetic data permits a greater flexibility with respect to the choice of values for the parameters and also eliminates any possible ambiguity associated with the measurement of chronopotentiometric transition times. Four principal models were considered. In the so-called *reacts first* model, it is assumed that the reaction of the adsorbed material proceeds to completion before the reaction of the solution material begins. This model predicts an *adsorption prewave* prior to the main chronopotentiometric wave. When two waves appear, $i_o\tau_1$ should be constant and $i_o\tau_2^{1/2}$ should also be constant. The sum of both transition times is denoted by τ and is related to the current density i_o and the charge density $nF\Gamma$ consumed by the reaction of the adsorbed material by the following expression[31-33]

$$nF\Gamma = i_o\tau - b^2/i_o \qquad (27)$$

where

$$b = nF\sqrt{\pi DC^*/2} \qquad (28)$$

Examples include the adsorption of phenylmercuric ion on mercury.[34]

Alternatively, the nondiffusing material might react at a *constant current efficiency* during the experiment.[32,35]

$$nF\Gamma = i_o\tau - b\tau^{1/2} \qquad (29)$$

The parameter b is defined by Equation 28. This model has been widely used in studies of the cooxidation of the electrode surface or the coreduction of surface oxide.[35-44] This is also the *split-current* model recommended by Noonan[54] to correct for the effects of double layer charging.

Third, the adsorbed material might not react until after the concentration of the material in the solution phase has been reduced to zero at the electrode surface. Under these conditions, two inflections should be observed in the chronopotentiometric potential-time curve, the second corresponding to an *adsorption postwave.* The sum τ of the two transition times is given implicitly for this *reacts last* model by [28, 33, 45]

$$\pi nF\Gamma = i_o\tau \arccos\left[\frac{2b^2}{i_o^2\tau} - 1\right] - 2[b^2(i_o^2\tau - b^2)]^{1/2}/i_o \qquad (30)$$

The parameter b is defined by Equation 28.

These three mechanisms are also known by the mnemonics AR, SR, (adsorbed reactant, solution reactant), SAR (solution and adsorbed reactant), and SR, AR (solution reactant, adsorbed reactant).

A fourth model considers that the extent of adsorption of material onto the surface of the electrode is proportional to the concentration in

the solution phase at the electrode surface and that the rates of the adsorption and desorption processes are so large that the solution and adsorbed species are in equilibrium at all times. Under this *equilibrium-linear isotherm* condition, the current densities and transition times are implicitly related by the following expression.[32, 33,48]

$$\Gamma(1-\exp a^2 \operatorname{erfc} a) = 2C^*\sqrt{\frac{D\tau}{\pi}} - \frac{nFC^{*2}D}{i_o} \qquad (31)$$

$$a = C^* \sqrt{D\tau/\Gamma}$$

The *modus operandi* used by Lingane [30] was to generate the synthetic data according to the first three of the models for several values of $nCD^{1/2}$ and $n\Gamma\Gamma$ and to analyze each set of data according to all four models. Least-squares methods for estimating these parameters from the data have been fully described.[30]

"Experimental errors" were introduced into synthetic transition time data by selection of 100 sequential normal deviates (*N. D.*) of zero mean and unit standard deviation and multiplication of these deviates by the appropriate percentage error *E*. Thus,

$$\tau_{exp} = (1+E \times N.D.)\,\tau_{theor} \qquad (32)$$

In this fashion, the generated data appear to be drawn from normal populations with uniform relative standard deviations. Because the distribution is normal, the χ^2 test[50] is applicable. The usual data set included one hundred (i,τ) values.

It is clear from these results that the χ^2 test is capable of distinguishing the model according to which the synthetic data were generated if the relative standard deviation of the transition-time data is less than about 1 or 2%.

Figure 4 illustrates the relative signs of the data residuals, that is the amount by which an individual "experimental" value of τ must be adjusted to force that data point to coincide with the least squares line, resulting from the analysis according to each of the models. The string designated as "true" corresponds to the experimental errors which were introduced into the data; this string would be unknown in an actual experimental study.

Considering first the 1% data, the signs of the residuals appear to vary in a random fashion only for the *reacts last* model, the model according to which the data were actually generated. The signs of the residuals calculated for the other models

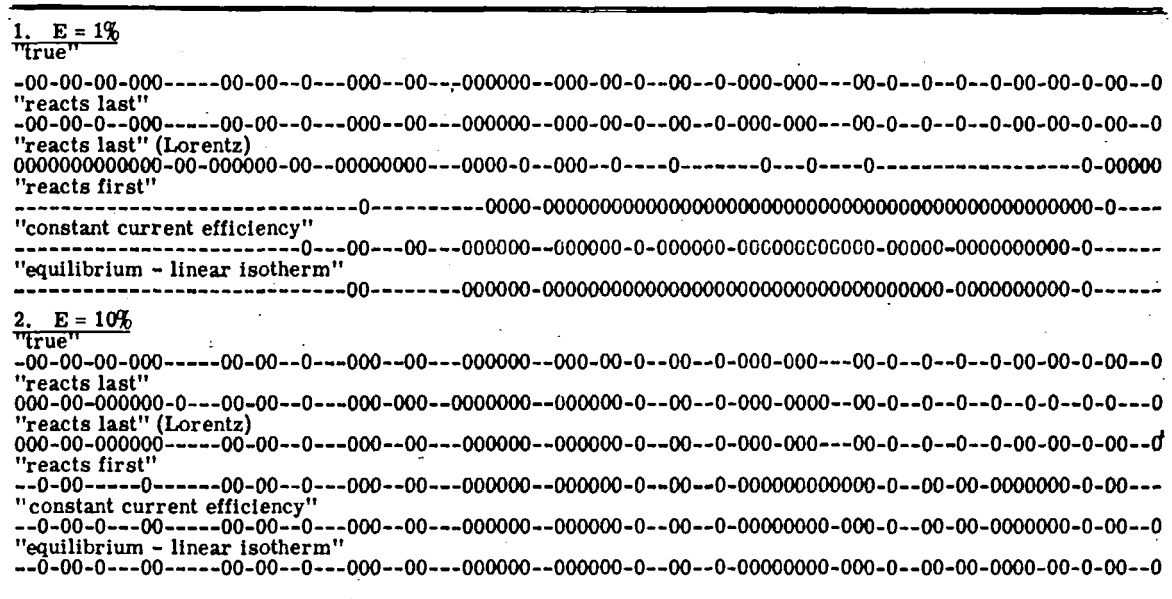

FIGURE 4. The relative signs of the residuals calculated for the individual values of . The data correspond to the "reacts last" model, $nCD^{1/2} = 2.5 \times 10^{-9}$ equiv/cm² sec$^{1/2}$ $n\Gamma\Gamma = 25\mu C/cm^2$. From Ref. 30. With permission.

exhibit distinct trends which indicate that the data fit these models less well.

With 10% data, it is no longer possible to state that the residuals calculated by one model vary in a more random fashion than those calculated for the others. We have achieved a situation where the experimental errors are large compared to the differences in the behavior indicated for the different models and this "fit" test is no longer applicable. It is for just this same reason that the χ^2 test does not distinguish among the different models at this level of experimental error. The results also indicate that the divergence among the values of the diffusion coefficient estimated according to the various models is largest in dilute solutions while the divergence among the estimated values of $n\mathrm{F}\Gamma$ is largest in the more concentrated solutions. As the solution concentration decreases, the estimated values of $n\mathrm{F}\Gamma$ fall into two classes: a class characteristic of the *reacts first* model and another class characteristic of the other three models. Therefore, if it is desired to obtain an approximate value for $n\mathrm{F}\Gamma$ in a dilute solution, it is of less consequence which model is chosen since the differences among the various models are probably no more than 25 to 50%. It is probably for this reason that the constant-current-efficiency model has been so useful for correcting chronopotentiometric data for the effects of electrode-surface oxidation and of double-layer charging and has permitted analytical applications[51] down to $10^{-6}M$.

Lingane demonstrated the following limited conditions under which it should be possible to use internal criteria to distinguish the most realistic chronopotentiometric model.

1. It must be demonstrated that the experimental transition times do not contain a bias, especially at high current densities, due to double-layer charging and other effects or that adequate procedures exist to correct the data for these effects.

2. A statistically meaningful method of data analysis and a data set of at least 25 to 50 points must be employed.

3. Sufficient replicates must be obtained at each data point to determine the standard deviation characteristic of that data point or to demonstrate the functional dependence of the standard deviation on the values of the transition time. It is mandatory that preliminary calculations be performed to determine that the weighting functions chosen are approximately valid under the given experimental conditions before these weighting functions are applied to the analysis of the experimental data.

4. The relative standard deviation of the transition-time data should be as small as possible and must be less than about 5%. This degree of precision is required since the differences between the various models are so slight. The 1% level needed for the application of the χ^2 test is probably not accessible except under the most auspicious circumstances.

5. The entire analysis must be repeated over a wide range of solution concentrations and the estimated values of the diffusion coefficient must be independent of this variation.

It should be clear that exceedingly large amounts of data would be required to determine the appropriate model, and accurate values for $n\mathrm{F}\Gamma$, in the fashion outlined here. To implement this program would be tedious.

Since it appears unlikely that one will usually be able to determine the actual model from chronopotentiometric data alone, about all one should expect of chronopotentiometry is a *range* of values for $n\mathrm{F}\Gamma$, corresponding to the results obtained by the application of limiting models. Noonan[54] has shown that one can go one step further and determine minimum and maximum values for $n\mathrm{F}\Gamma$. His approach involves the definition of the following dimensionless variables.

$$\alpha = 4i_o^2\,\tau/[nFC^*\sqrt{\pi D}]^2$$

$$\beta = i_o\,\tau/nF\Gamma$$

Note that α is simply the square of the ratio of the observed chronopotentiometric constant ($i_o\tau^{1/2}/C^*$) to the value predicted by the Sand Equation and that β is the ratio of the total charge to the charge consumed by the reaction of the adsorbed species.

Theoretical curves are prepared by expressing the model in terms of α and β and then plotting $\log \alpha$ as a function of $\log \beta$. The experimental data are treated by plotting $\log i_o^2\tau/C^{*2}$ against $\log i_o\tau$. If the model is accurate, the experimental and theoretical curves can be superimposed simply by vertical and horizontal translations. When superimposed, the experimental values of $i_o^2\tau/C^{*2}$ will correspond to specific values of α and, correspondingly, the experimental values of $i_o\tau$ will correlate with specific values of β. In this way, values of $nCD^{1/2}$ and of $n\mathrm{F}\Gamma$ may be calculated.

If one assumes no interconversion of adsorbed and solution species during the experiment, then the *reacts first* model is the *maximum model* and the *reacts last* model the *minimum model*; that is, for a given chronopotentiogram whose transition time is lengthened by the reaction of adsorbed material, the *reacts first* model will yield the largest value for nFΓ and the *reacts last* model the minimum value for nFΓ. In terms of α and β these models are

reacts first: $\alpha = \beta/(\beta-1)$.

reacts last:

$$\arccos\left(2/\alpha-1\right)-\sqrt{(\alpha-1)/\alpha^3} = \pi/\beta$$

These two limiting cases are plotted (log α vs. log β) as curves B and C in Figure 5. Any other model which assumes no interconversion of diffusing and adsorbed species must fall somewhere between these two parametric curves.

If there is interconversion between adsorbed and diffusing species, it can be shown[54] that a given nFΓ will have maximum effect in the physical situation in which the equilibrium shifts, at the start of electrolysis, to very strongly favor adsorption. During electrolysis, any material diffusing to the electrode is immediately adsorbed, i.e., C(x=0) = 0, and the adsorbed material reacts electrochemically at a rate determined by i_o. Such a system might be realized for a neutral species which is reduced near the electrocapillary maximum, if the initial potential is considerably anodic to the electrocapillary maximum. When calculating nFΓ from experimental data according to this hypothesis, one obtains the *minimum estimate* for nFΓ.

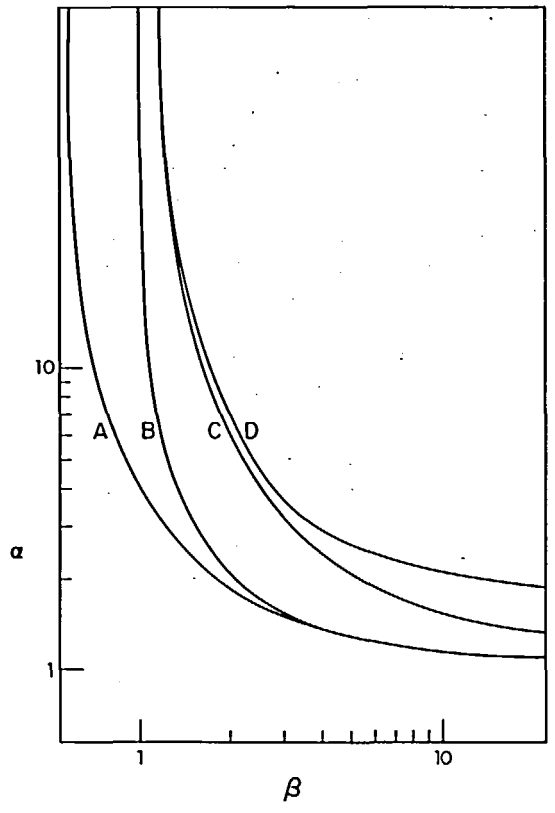

FIGURE 5. Parametric plots of theoretical adsorption models. A. Maximum nFΓ. B. Adsorbed reacts first. C. Adsorbed reacts last. D. Minimum nFΓ. Redrawn from Ref. 54. With permission.

This model is of a form similar to the constant-current-efficiency model, Equation 29.

$$\text{fully adsorbed} \quad i_o\tau = nF\Gamma + 2nFC^* \sqrt{D\tau/\pi}$$

$$\alpha^{1/2} = \frac{4}{\pi}\,\beta/(\beta-1)$$

One unexpected feature of this model is the low current density limit. It has been tacitly assumed that all effects of adsorption disappear at long transition times; that is, that all adsorption models reduce to the Sand Equation at sufficiently long transition times. Yet this model predicts that, in the long transition time limit, the value of $i_o \tau^{1/2}/C^*$ will differ by a factor of $\pi/4$ from the value that one would expect in the absence of adsorption! Thus, constancy of $i_o \tau^{1/2}/C^*$ at long times is a necessary but not sufficient condition that the reacting species is unadsorbed.

The maximum model, when there is interconversion of adsorbed and diffusion species, occurs[54] when the adsorbed material fully desorbs at the very start of electrolysis. This realistic possibility[28, 52, 53] is characteristic of the Zn^{+2} SCN^- system.[52,53]

$$\text{fully desorbed} \quad 2i_o\tau = nFC^* \sqrt{\pi D\tau} + nF\Gamma$$

$$\alpha^{1/2} = 2\beta/\left|2\beta-1\right|$$

Note that this model is functionally similar to the constant current efficiency model but with a factor of two introduced in the nFΓ term.

The minimum and maximum models, including interconversion, are plotted as curves A and D of Figure 5. These two curves describe the boundaries for all adsorption models, no matter how unique the form of the model equation. Although these models are based on radically different physical pictures of the adsorption process, the parametric

plots are very similar. This is further evidence of the difficulty in distinguishing the correct model from chronopotentiometric data alone.

These parametric plots are recommended for those situations in which the model is unknown because it permits the experimenter a good "feel" of the magnitude of the adsorption effect. If the model is known, the least-squares method[30] is superior because it estimates the error in the derived quantity. In both cases, an independent estimate of the diffusion coefficient is strongly recommended. In the log-log plots, for example, an independent estimate of the diffusion coefficient permits an unambiguous positioning of the data on the log α axis.

Murray[46] has described criteria under which ramp-current and step-current chronopotentiometry might be used to distinguish among common adsorption models. Reverse-current chronopotentiometry[114] has been applied to the determination of adsorption parameters. Thin-layer chronopotentiometry[4] offers an elegant approach to the determination of $n\Gamma$.

IV. THE DETERMINATION OF THE CHRONOPOTENTIOMETRIC TRANSITION TIME

Because the potential of the working electrode changes during a chronopotentiometric experiment, a certain portion of the applied current is always consumed not in the faradaic process but in providing the additional charge necessary to keep the charge density on the electrode surface in equilibrium with the values appropriate to the new potentials. This capacitive current is assumed to be given by an expression of the following form where C_{dl} is the differential double layer capacitance.

$$i_c = \frac{d}{dt}(C_{dl}\, E) \qquad (33)$$

Since the charging current depends on the slope of the potential-time curve, it will be largest at the beginning and at the end of the chronopotentiograms.

One way to minimize the effects of double-layer charging is to feed back to the summing point of the control amplifier, in a circuit like that of Figure 3C, a signal proportional to dE/dt. This amounts to assuming a constant double-layer capacity. Success cannot be claimed for such an approach.[136]

An analogous approach[55] is to use two cells. The potential of the working electrode in a reference cell containing no electroactive material is made to "track" the potential of the working electrode in the cell containing electroactive material. Any current that flows in the reference cell is added electronically to the current flowing through the working cell. The basic premise upon which such a compensation network is based is that the currents due to extraneous processes are not influenced by the presence of electroactive material. This is equivalent to assuming that the double-layer capacity does not depend on the electroactive material, an assumption that is not always clearly valid, especially if there is adsorption of the electroactive species.[56]

The distortion of the chronopotentiometric potential-time curve has received considerable theoretical attention.[6, 57-59] All authors have assumed the double layer capacity to be independent of potential. Rodgers and Meites[57] used a "brute force" numerical method to solve the Fick's law equations. DeVries[58] formulated the problem as a nonlinear integral equation in terms of the surface concentrations of the electroactive species, and Olmstead and Nicholson[59] formulated the problem as a nonlinear integral equation in which the capacitive component of the current is the function to be determined. This last approach would appear to be most successful as the numerical solutions are obtained most readily. Rodgers and Meites[57] treated both reversible and irreversible systems, Olmstead and Nicholson only reversible systems.[59] Although at first glance the chronopotentiograms calculated by these two groups appear to be of quite different shape, this apparently is only an artifact introduced by the considerably expanded time axis used by Rodgers and Meites[57] in drawing their figures. Note that the parameters in terms of which these authors express their respective results differ by a multiplicative factor of RT/F or about 0.03 V at room temperature.

Typical theoretical chronopotentiograms for a reversible system are illustrated in Figure 6 for both forward and reverse current chronopotentiometry. The double layer distortion parameter ψ_{dl} is defined by Equation 34.

$$\psi_{dl} = \frac{RT}{nF}\frac{4i_o C_{dl}}{(nFC^*\sqrt{\pi D})^2} \sim \frac{RT}{nF}\frac{2C_{dl}}{nFC^*\sqrt{\pi D\tau}} \sim \frac{RT}{nF}\frac{C_{dl}}{i_o \tau} \qquad (34)$$

where i_o is the total current density, C_{dl} is the double layer capacitance, τ is the correct, i.e., unenhanced, transition time, and RT/F has a value of 25.6 mV at room temperature.

The transition time for a given value of the distortion parameter ψ_{dl} depends inversely on the *square* of the bulk concentration. For example, for a solution of a substance with ordinary values for its diffusion coefficient (10^{-5} cm^2/sec) and double layer capacitance (20μ Farads cm^{-2}), the transition time is about $3\times10^{-18}/(nC^*\psi_{dl})^2$. Consequently, one tries to use as large a concentration as possible to minimize distortion. If one takes $\psi_{dl} < 0.005$ as the limit for a minimally distorted chronopotentiogram, and if one takes ten seconds as the longest practical transition time, one concludes that the lower limit for *practical* analytical applications is at about the 0.1 m*N* concentration level. Well-defined chronopotentiograms have been obtained for the reduction of 0.015 m*N* Pb^{++}, however, by using long (~50 seconds) transition times.[61] If one assumes a potential change of 200 mV, the ratio of the change in double-layer charge to the charge consumed by the faradaic process is about four at 0.1 m*N*. The optimum range is 1 to 10 m*N*.

There are basically four distinct methods that have been employed to measure transition times and to correct for the effect of double-layer charging. Many authors[61, 62] have obtained their data by measuring the transition time from the beginning of electrolysis to a preselected *transition potential* in the vicinity of the inflection point. This method is easily automated by constructing a voltage comparator circuit to "flip" at the transition potential. Such a circuit is a key element in instrumentation for *cyclic chronopotentiometry*.[25] Excellent results are obtained so long as one avoids short transition times, i.e., large values of ψ_{dl}.

Electronic differentiation of chronopotentiometric potential-time curves has been proposed[63, 64] for transition-time determination. As may be seen in Figure 7, the derivative has two maxima

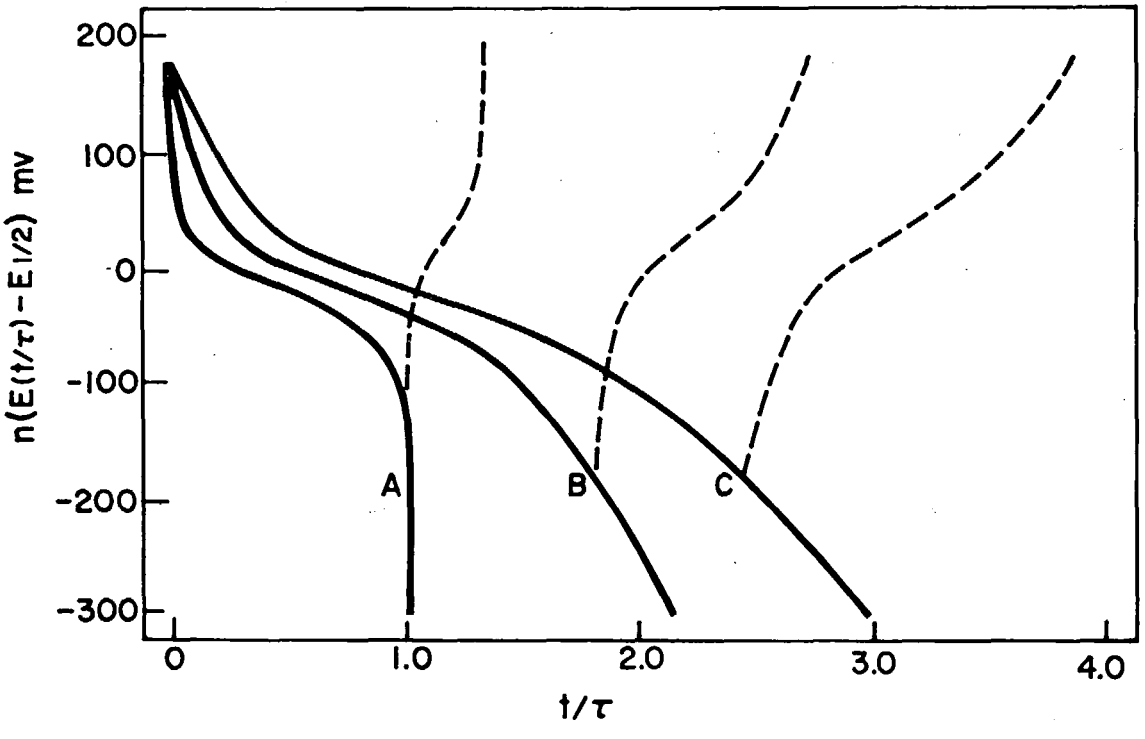

FIGURE 6. Calculated chronopotentiograms distorted by double layer charging. Dashed lines are after current reversal. y = t/τ, whereτ is the unenhanced transition time. ψ_{dl} = A, 0.0; B. 0.03; C, 0.06. From Ref. 59. With permission.

and the interval between these maxima is a measure of the transition time. Peters and Burden[64] have established that the magnitude of dE/dt at the *minimum* is quantitatively related to the transition time for both reversible and irreversible electrode processes and, thus, can be use as a direct and unempirical measure of the transition time. For example, for a reversible process at 25°

$$\tau = -\frac{27}{8}\frac{RT}{nF}\left(\frac{dE}{dt}\right)^{-1}_{min} = \frac{-0.0866}{n}\left(\frac{dE}{dt}\right)^{-1}_{min} \qquad (35)$$

The hope was that this method might be less sensitive to double-layer charging and that it might, therefore, be applicable to lower concentrations (larger ψ_{dl} values); this hope has not been

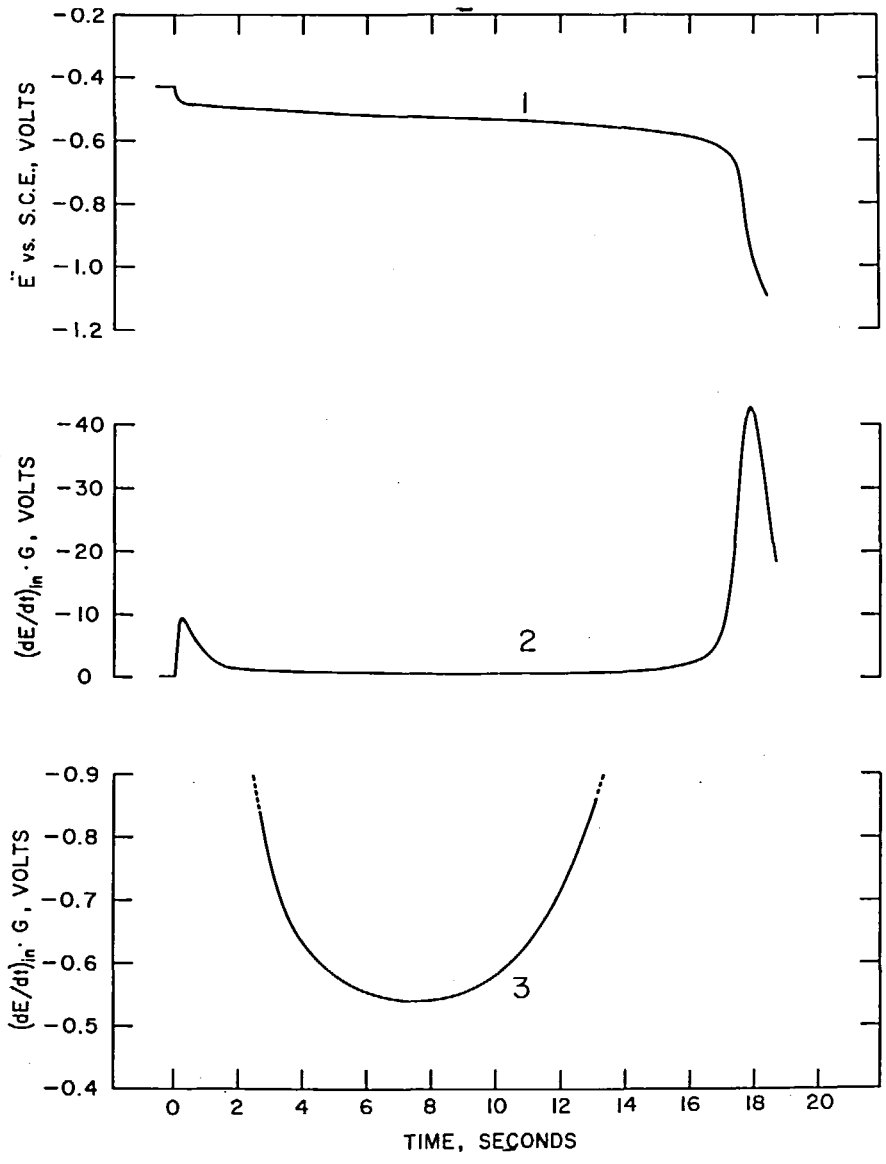

FIGURE 7. Curve 1. Conventional chronopotentiogram for reduction of 6.28 m*M* thallium(I) in 0.1F potassium nitrate at mercury pool cathode; $i_o = 364\ \mu A/cm^2$. Curve 2. Derivative chronopotentiogram corresponding to Curve 1. Curve 3. Derivative chronopotentiogram showing magnified portion of Curve 2 near the region of the minimum. From Ref. 64. With permission.

realized. Peters and Burden[64] concluded that "derivative chronopotentiometry is slightly, but not greatly, superior to conventional chronopotentiometry in providing better constancy of $i_o\tau^{1/2}/C$ as the concentration of the electroactive substance is decreased."

The theoretical relationships for programmed current derivative chronopotentiometry have been derived[65] but they appear to be of even less practical utility.

Generally speaking, one of a variety of graphical methods gives better results at high i_o/C^* ratios (short transition times, large ψ_{dl}), than either of the above methods. The principal graphical methods are delineated in Figure 8. The usual criterion for acceptability has been that measured values of $i_o\tau^{1/2}/C^*$ are constant over a wide range of current densities and concentrations.

Russell and Peterson[70] were the first to attempt to refine this criterion by comparing the transition times evaluated by the methods of Delahay and Berzins,[66] of Reinmuth,[6] and of Kuwana[67] (the methods of Reinmuth and Kuwana are illustrated in Figure 8) with the value obtained by fitting the data to an expression of the form of Equation 25 for the irreversible reduction of iodate at a mercury electrode in an alkaline solution. Some of their results appear in Table 1.

TABLE 1

Comparison of Transition Times by Different Methods (Variability in least-squares τ is due to changes in current density.)[70]

Least Squares	Delahay and Berzins	Reinmuth	Kuwana
6.83*	6.64	6.69	6.79
6.84	6.44	6.54	6.75
6.81	6.61	6.67	6.82
6.80	6.60	6.65	6.82
6.94	6.75	6.80	6.96
6.86	6.69	6.74	6.88
6.62	6.39	6.45	6.65
6.65	6.45	6.54	6.68

*Seconds.

Their conclusion was that the method of Kuwana gave the best agreement. It should be emphasized, however, that this conclusion is restricted to very specific conditions: a totally irreversible wave and six-second transition times ($\psi_{dl} = 0.0003$).

With theoretical distorted chronopotentiograms in hand, it is possible to test the various methods of transition time measurement. The independent conclusion of Rodgers and Meites[57] and of Olmstead and Nicholson[59] is that the graphical methods fail, with the possible exception of the method of Laity and McIntyre[69] (cf. Figure 8). Some of the results of Olmstead and Nicholson[59] appear in Table 2.

TABLE 2

Normalized Transition Times Determined by (A) Method of Delahay and Berzins, (B) Method of Reinmuth and (C) Method of Laity and McIntyre.

ψ dl	τ meas/τ true		
	A	B	C
0.005	1.017	1.056	0.989
0.01	1.042	1.100	0.979
0.02	1.088	1.175	0.974
0.03	1.128	1.240	0.972
0.04	1.165	1.298	0.970
0.06	1.231	1.401	0.968
0.08	1.289	1.493	0.967
0.10	1.342	1.576	0.966

The accuracy of the several graphical techniques has been studied in some detail experimentally by Noonan and Reinmuth.[54] This work has not been widely disseminated which is unfortunate as it is one of the very best discussions of the influence of double-layer charging on chronopotentiometry. Noonan[54] studied the system Cd^{++} in $2M$ KNO_3 at a mercury electrode at ψ_{dl} values up to 0.1 and concluded that no simple fixed-potential or graphical measurement technique is adequate to correct the transition times under these conditions. Some of his data appear in Table 3. Note that the Laity-McIntyre method, while better than the Reinmuth method, is imprecise and yields a rather small value for the diffusion coefficient of Cd^{++}.

Variations of the fixed potential method would appear to be the best practical approach to the determination of accurate $i_o\tau^{1/2}/C^*$ data. There are two basic approaches that have been suggested. Rodgers and Meites[57] and Olmstead and Nicholson[59] independently suggested that the time required for the potential to traverse a fixed interval, measured with respect to $E_{1/2}$, could be corrected empirically by comparison with theoretical chronopotentiograms. For example, one might measure the time from a point 120/n mV before $E_{1/2}$ to a point 160/n mV after $E_{1/2}$ (cf. Figure 8A). Assuming $\psi_{dl} \sim 0.03$, one would divide this time by 1.65[59] to obtain an estimate of the true transition time. A considerable wealth of correc-

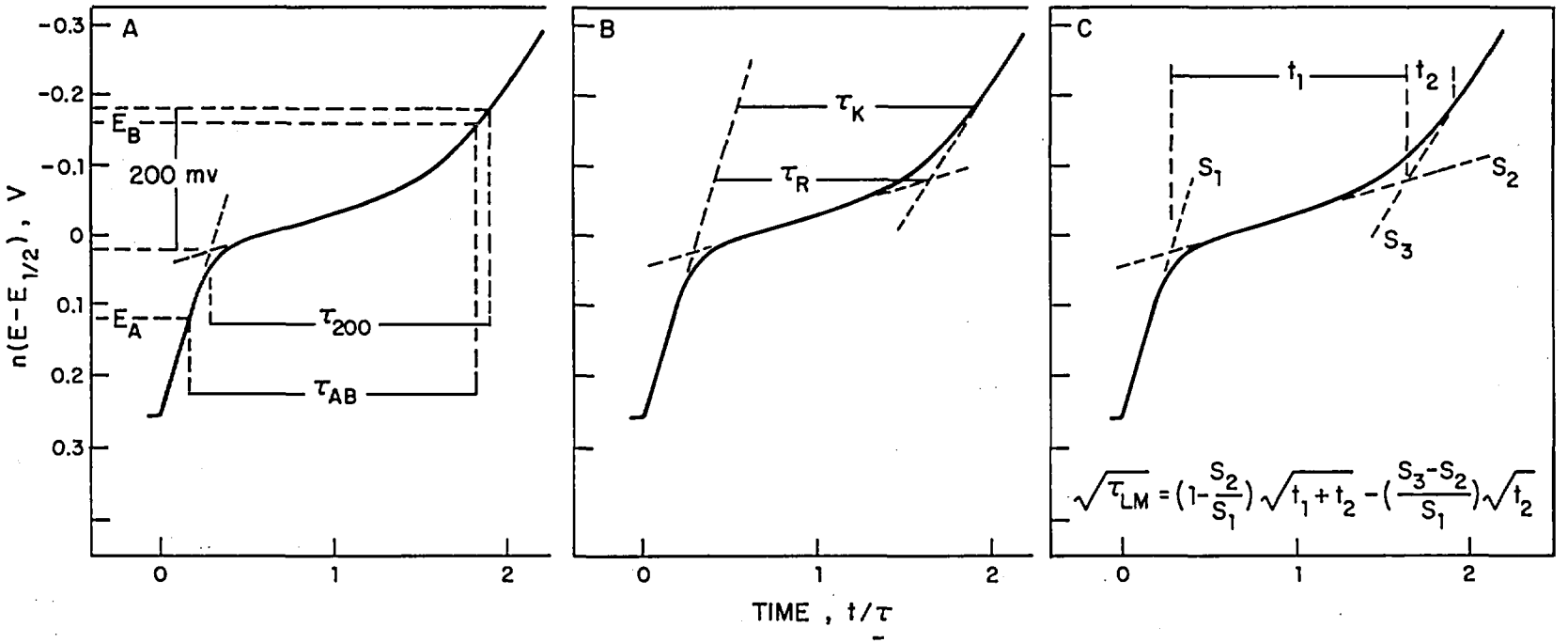

FIGURE 8. Principal methods of transition time measurement. The E-t curve is drawn for a reversible system, $\psi_{dl} \sim 0.03$ and is plotted as a function of t/τ, where τ is the unenhanced transition time. A. Measurement between fixed potentials. τ_{AB} is the time interval between two potentials chosen with respect to $E_{1/4}$, τ_{AB} is corrected by empirical factors[57,59] which depend on the potentials chosen for E_A and E_B and on the value of ψ_{dl}; τ_{200} is the time interval between the potential at the intersection of the two tangents and a potential 200 mV cathodic (anodic). Noonan[54] recommends correcting τ_{200} according to the SAR model. B. Transition time is measured from the extrapolated initial trace to the point of intersection of tangents drawn to the middle and final portions of the E-τ curve, method of Reinmuth,[6] or to the point of collinearity of the final tangent with the E-t curve, method of Kuwana.[67] C. Method of Laity and McIntyre.[69] S_1, S_2, and S_3 represent the slopes of the initial, middle, and final portions of the E-t trace.

TABLE 3

Values of $i_o\tau^{1/2}/C$,* Corrected for Double Layer Charging by Several Techniques, for the System 1 m*M* Cd^{++}, in 2 *M* KNO_3.[54]

i_o mamp/cm²	200 mV	200 mV + SAR	Reinmuth	Laity-McIntyre
3.40[a]	542	500	517	450
4.26	553	502	512	425
5.65	566	500	529	408
6.74	571	493	–	–
8.42	582	487	–	–
9.32	593	500	556	421
10.5	609	495	576	388
12.0	624	497	578	402
12.9	631	497	571	422
14.0	643	500	602	394
15.2	653	499	605	395
16.7	665	499	597	400
18.4	671	490	634	389
20.9	701	505	602	426
23.9	711	488	626	440
28.1	746	498	648	418
33.6[b]	780	496	681	450

[a] $\psi dl \sim 0.01$

[b] $\psi dl \sim 0.1$

tion factors is included in these two sources for both reversible and irreversible systems. The validity of this approach has been shown[60] experimentally for the reversible reduction of ferric iron in an oxalate buffer for ψ_{dl} values up to 0.1, the maximum investigated.

Noonan[54] also recommends measuring the time interval between two fixed potentials but he corrects the data for double-layer charging by the constant-current-efficiency model (the SAR model), using an independently determined estimate of the double layer capacitance. This method is illustrated in Figure 8 and is essentially a modification of a method originally proposed by Bard.[36] As may be seen by a comparison of columns two and three of Table 3, this method leads to a very constant value of $i_o\tau^{1/2}/C^*$. The diffusion co-efficient calculated from these data is 8.4×10^{-5} cm²/sec for Cd^{++} in 2 *M* KNO_3.

Olmstead and Nicholson[59] had attempted to plot the time between fixed potentials from calculated chronopotentiograms according to the constant-current-efficiency model and had observed a good correlation for only one specific set of initial and final potentials and for this reason discarded this approach. However, Noonan's[54] approach utilized the intersection of the initial tangent with the tangent at $E_{1/2}$ as the initial potential and in this way entirely excluded the initial portion of the potential-time curve where double-layer charging is the major process. This probably explains why Noonan succeeded where Olmstead and Nicholson failed.

Since either of these fixed-potential methods appears to permit the determination of accurate transition time data at ψ_{dl} values as large as 0.1, we probably should revise downward our earlier estimate of the lowest concentration for analytical applications. Under the same assumption as before, a concentration of 0.005 millinormal corresponds to $\psi_{dl} = 0.1$ for a ten-second transition time. This has been achieved.[51]

Finally, DeVries' comments on the effect of double-layer charging on programmed-current chronopotentiometry ($i = Bt^{1/2}$, $Bt^{3/2}$) are of interest. He concludes[71] that whatever the slight advantages of this technique†, they are nullified by the more complex effects of double-layer charging.

V. CHRONOPOTENTIOMETRIC TRANSITION TIMES AT CYLINDRICAL, SPHERICAL AND UNSHIELDED PLANAR DISC ELECTRODES

Chronopotentiometry at a shielded planar electrode is inconvenient because of the difficulty in renewing the solution close to the electrode between experiments. However, chronopotentiometry at cylindrical wire electrodes or at unshielded planar disc electrodes or at spherical hanging mercury drop electrodes is restricted to short-time intervals lest the curvature of the electrode or nonperpendicular diffusion (edge effects) invalidate the Sand Equation.[73] The cylindrical-electrode analog of the Sand Equation is[43]

$$i_o\tau^{1/2}/C^* = nF\sqrt{\pi D}/2R \qquad (36)$$

†When $i = Bt^{1/2}$, the measured transition time is proportional to the bulk concentration and this has been suggested as an advantage for analytical applications.[72,115] However, the *precision of a concentration measurement* is only half that of conventional chronopotentiometry, assuming that the transition time can be measured with equal precision in the two cases.

where $R = 1. - 0.443Q + 0.255Q^2 - 0.167Q^3 + 0.132Q^4 - 0.125Q^5 + 0.142Q^6 - 0.187Q^7 + 0.528Q^8 + ..$

and $Q^2 = D\tau/r^2$

r is the radius of the cylindrical wire electrode. Tables of 1/R have been calculated.[74]

The series of terms represented by R in the denominator of the Sand Equation is convergent initially for $D\tau/r^2$ less than unity but becomes divergent after the sixth term. However, this is no real handicap because for a wire of radius 0.02 cm, a smallish value, and $D = 2 \times 10^{-5}$ cm/sec, an unusually large value, the value of $D\tau/r^2$ is less than unity for transition times shorter than about 20 seconds. Nonetheless, the theory has been extended[75] to permit the calculation of values of 1/R for larger values of $D\tau/r^2$ and agreement was found for previously published data for the reduction of hydrogen ion at a platinum wire electrode.[76]

It is very fortunate that one does not need to use this rather bulky expression if one's interest lies in evaluating the chronopotentiometric constant $i_o\tau^{1/2}/C^*$ because it has been discovered empirically[76] that the effects of the cylindrical geometry can be adequately accounted for by extrapolating the observed values of $i_o\tau^{1/2}/C^*$ to the intercept at $\tau^{1/2} = 0$ (Figure 9). No one has yet justified this equation theoretically.

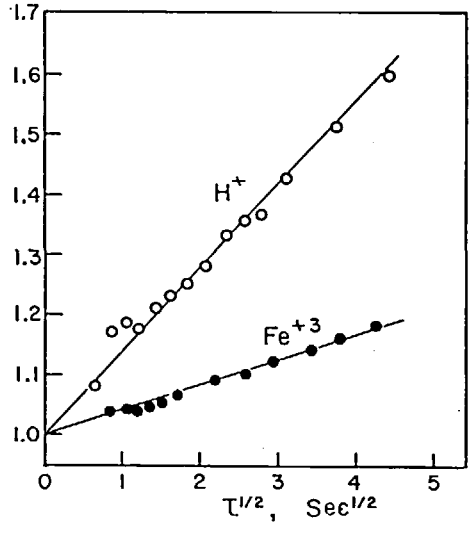

FIGURE 9. The chronopotentiometric constant as a function of $\tau^{1/2}$ at a cylindrical wire electrode of radius 0.025 cm. The ordinate has been normalized in both cases by dividing the data by the respective intercept values. From Ref. 76. With permission.

$$i_o\tau^{1/2}/C^* = \frac{nF\sqrt{\pi D}}{2}\left(1 + B\sqrt{\frac{D\tau}{r^2}}\right) \quad (37)$$

An entirely analogous relationship has been observed[77] in chronopotentiometric experiments carried out with an unshielded planar disc electrode (cf. Figure 10). Here, the slope B has a value very close to unity and r represents the radius of the disc electrode. In this case it can be shown[78] that this is the theoretical relationship.

The Sand Equation analog appropriate to spherical geometry was first obtained by Mamantov and Delahay[79]

$$\frac{nFC^*}{i_o}\frac{D}{r} = 1 - \exp\left(\frac{D\tau}{r^2}\right)\operatorname{erfc}\sqrt{\frac{D\tau}{r^2}} \quad (38)$$

where r is the radius of the sphere. Expanding the right-hand side of this equation for small values of $D\tau/r^2$ (≤ 0.023), one obtains an expression closely analogous to that for a cylindrical electrode

$$i_o\tau^{1/2}/C^* = nF\sqrt{\pi D}/2R \quad (39)$$

where $R = 1 - \sqrt{\pi D\tau}/2r + 2D\tau/3r^2 ...$

Values of R have been tabulated.[80]

For typical values of the parameters ($r \sim 0.06$ cm; $D^{1/2} \sim 0.003$ cm/sec$^{1/2}$), $D\tau/r^2 = 0.023$ corresponds to a transition time of some nine seconds. This is longer than normally used with hanging mercury electrodes because unstable density gradients and other stirring effects become important. Therefore, the approximation inherent in Equation 39 is valid over the region of interest.

Since the third term in R is small, $i_o\tau^{1/2}/C^*$ for spherical electrodes is very nearly a linear function of $\tau^{1/2}$ as it is for unshielded disc electrodes and for cylindrical electrodes. Therefore, from the practical analytical point of view, and for the determination of diffusion coefficients, the recommended procedure is to extrapolate the measured $i_o\tau^{1/2}/C^*$ data to the intercept at $\tau^{1/2} = 0$ when working with any of these electrode geometries. Note that if $i_o\tau^{1/2}$ is essentially constant, a plot of $i_o\tau^{1/2}$ vs. $\tau^{1/2}$ is of the same form as the $i_o\tau^{1/2}$ vs. $1/i_o$ plots

used to detect a homogeneous chemical reaction preceding electron transfer.

Numerous studies with the Kemula-type hanging mercury drop electrode have shown that quite constant values of $i_0\tau^{1/2}/C^*$ are obtained up to transition times of three to five seconds, although Equation 39 predicts about an 8% error at four seconds. This failure of experiment and theory occurs[80] because the treatment neglects the fact that diffusion away from the drop is not truly spherically symmetrical due to the close proximity of the blunt glass capillary. This is analogous to one of the reasons for failure of the Ilkovič equation in polarography.[81] The diffusion volume excluded by this capillary apparently is sufficiently large that, for transition times of the order of a second or so, it largely compensates for the increase in diffusion volume provided by the spherical geometry. By grinding the capillary tip to a point, Jones[80] was able to achieve good agreement between theory and experiment.

A similar effect has been reported by Murray and Gross for current reversal at a hanging mercury drop electrode.[82]

An ingenious experimental method for correcting for the cylindricity effect was proposed by Kuempel and Schaap.[83] These authors noted that the problem of diffusion to the inside surface of a hollow cylinder is simply the mirror image of diffusion to the surface of a solid cylinder. Therefore, as may be seen in Figure 11, Curve C, $i_0\tau^{1/2}/C^*$ *decreases* at long transition times for diffusion to the inner surface of a hollow cylinder, and this behavior nearly exactly mirrors the *increase* in $i_0\tau^{1/2}/C^*$ at a solid cylindrical electrode of the same radius, curve A. Kuempel and Schaap[83] suggested that the deviations due to the contracting (in the case of the hollow cylinder) and expanding (solid cylinder) diffusion fields would largely cancel if two electrodes of equal radius and area were used in parallel. Curve B, and similar data for the reduction of $Fe(CN)_6^{-3}$ and Ag^+, demonstrates their hypothesis to be correct. This setup might be advantageous for analytical applications where long times make transition-time measurement easiest ($\psi_{dl} \rightarrow 0$) because it is doubtless somewhat easier to flush and refill this electrode combination than to flush and refill a shielded planar electrode.

Recently, Sheaffer and Peters[84] have used *concentric* cylindrical electrodes of nearly the same radius for thin-layer chronopotentiometric

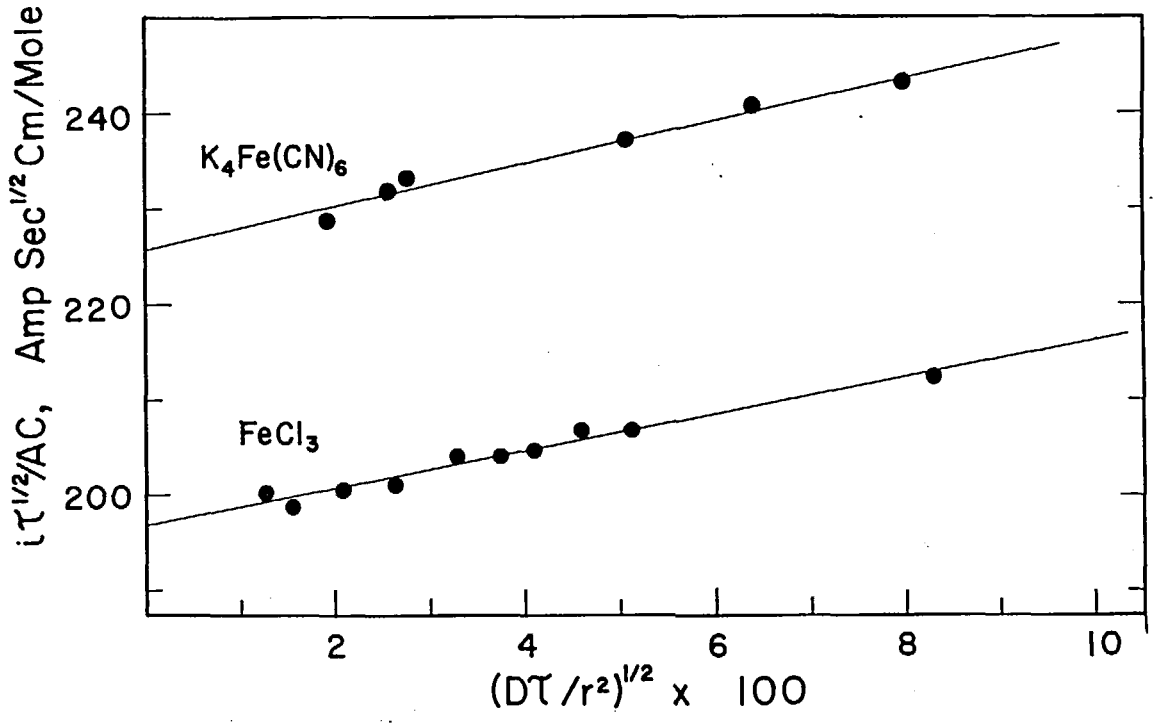

FIGURE 10. The chronopotentiometric constant as a function of $(D\tau)^{1/2}$ at an unshielded planar disc electrode of radius ρ. From Ref. 77. With permission.

experiments. Electrolysis under these conditions followed Faraday's law, $i\tau = nFCV$, where V is the solution volume. The advantages of this combination over other thin-layer designs[4] are simplicity and accessibility of the electrode for cleaning and/or preconditioning of the electrode surface. Since the electrolysis products may be discharged into a 0.1-mm quartz plate spectrophotometric cell, this is one of the more convenient designs for the spectrophotometric identification of stable products.

VI. CHRONOPOTENTIOMETRIC E-T CURVES AT CYLINDRICAL ELECTRODES

We saw in an earlier section that the chronopotentiometric potential-time curve for the reversible redox system $O + ne = R$, with both species soluble and no complicating solution reactions, is given by Equation 23. Since the shape of the experimental potential-time curve is often used as a criterion for the reversibility of the electrode reaction, it is of interest to consider how these equations should be modified if we are using a cylindrical wire electrode rather than the shielded planar electrode for which they were derived. Let us introduce the quantity Θ.

$$\Theta(r,t) = t^{\frac{1}{2}}[1.-0.443Q + 0.255Q^2 - 0.167Q^3 + \ldots]$$

where

$Q^2 = D\tau/r^2$ r is the electrode radius.

It can be shown that the concentrations of O and of R at the wire electrode *surface* are given by

$$C_O(r,t) = \frac{2i_o}{nF\sqrt{\pi D}}[\Theta(r,\tau)-\Theta(r,t)] \quad (40)$$

$$C_R(r,t) = \frac{2i_o}{nF\sqrt{\pi D}}\Theta(r,t) \quad (41)$$

$D_O = DR = D$.

The potential-time curve is obtained as usual by substitution of these expressions into the Nernst Equation. $E_{1/2}$ is the polarographic half-wave potential.

$$E = E_{\frac{1}{2}} - \frac{RT}{nF}\ln\left[\frac{\Theta(r,t)}{\Theta(r,\tau)-\Theta(r,t)}\right] \quad (42)$$

The ratio of t^*/τ, where t^* is the time at which the logarithmic term is unity, and the value of $E(t^*) - E_{1/2}$ were evaluated for several values of $D\tau/r^2$ and the results appear in the accompanying table.

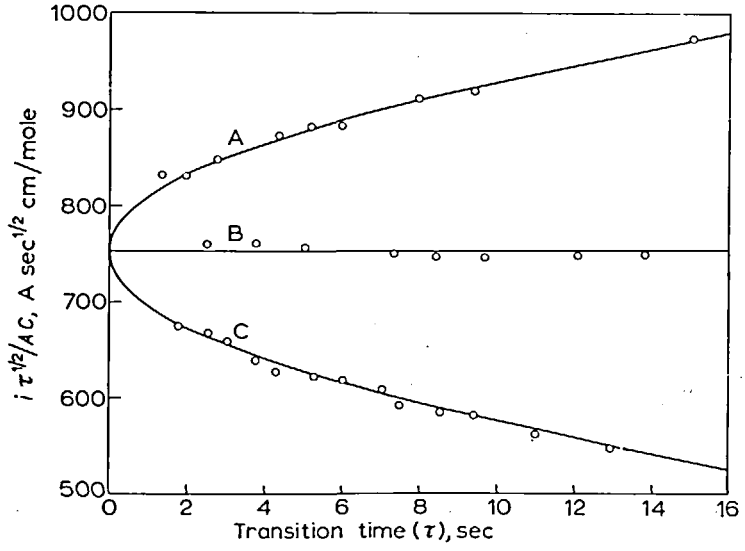

FIGURE 11. The chronopotentiometric constant as a function of τ for the reduction of H^+ at A, a wire electrode; C, a hollow cylindrical electrode; and B, wire and hollow cylindrical electrodes simultaneously. From Ref. 83. With permission.

TABLE 4

$\frac{D\tau}{r^2}$	τ, seconds	t^*/τ	$E(t^*) - E_{1/2}$, mV
0.0178	1	0.235	0.7 /n
0.0712	4	0.225	2.7
0.160	9	0.221	3.6
0.445	25	0.194	7.4
0.523	9	0.185	7.1

The results of these calculations indicate that the quarter-wave potential, $E(\tau/4)$, obtained with a cylindrical electrode should differ by no more than a few millivolts from the polarographic half-wave potential; hence the effect of cylindricity is, for all practical purposes, negligible.[137]

A plot of $\ln[\theta(r,t)/(\theta(r,\tau)-\theta(r,t))]$ versus $\ln[\sqrt{\tau/t} - 1]$ indicates that when chronopotentiograms obtained with cylindrical electrodes are analyzed in the usual way by plotting E(t) vs. $\log [\sqrt{\tau/t} - 1]$ one would expect to observe straight lines whose slopes are only slightly increased from the shielded planar electrode value of $\frac{0.059}{n}$V.[137]

Presumably, arguments could be developed to reach similar conclusions at unshielded disc and spherical electrodes.

VII. MIXTURES AND STEPWISE REACTIONS

Although the current efficiency becomes less than 100% immediately at the transition time, the current efficiency for the first process remains high for a considerable period. Consequently, the current consumed by the second process is smaller than the total applied current during this period and the transition times for the second and subsequent species are lengthened over the values that would be predicted by an unthinking application of the Sand Equation.[1, 7, 23]

An example of this effect is shown in Figure 12. The Cu(II) → Cu(I) wave is considerably enhanced in the presence of the more easily reduced Fe(III) since the effective current density for the reduction of Cu(II) is less than that in the absence of iron because of the continuing reduction of the iron after the first transition time.

A similar effect holds for the stepwise reduction of a single substance; the Cu(I) → Cu(0) wave is lengthened, even in the absence of iron, because of the continuing reduction of Cu(II). In the case of a stepwise process, the production of the intermediate, in this case Cu(I), does not cease at the first transition time. The flux of Cu(I) at the surface of the electrode, i.e., the rate at which it is

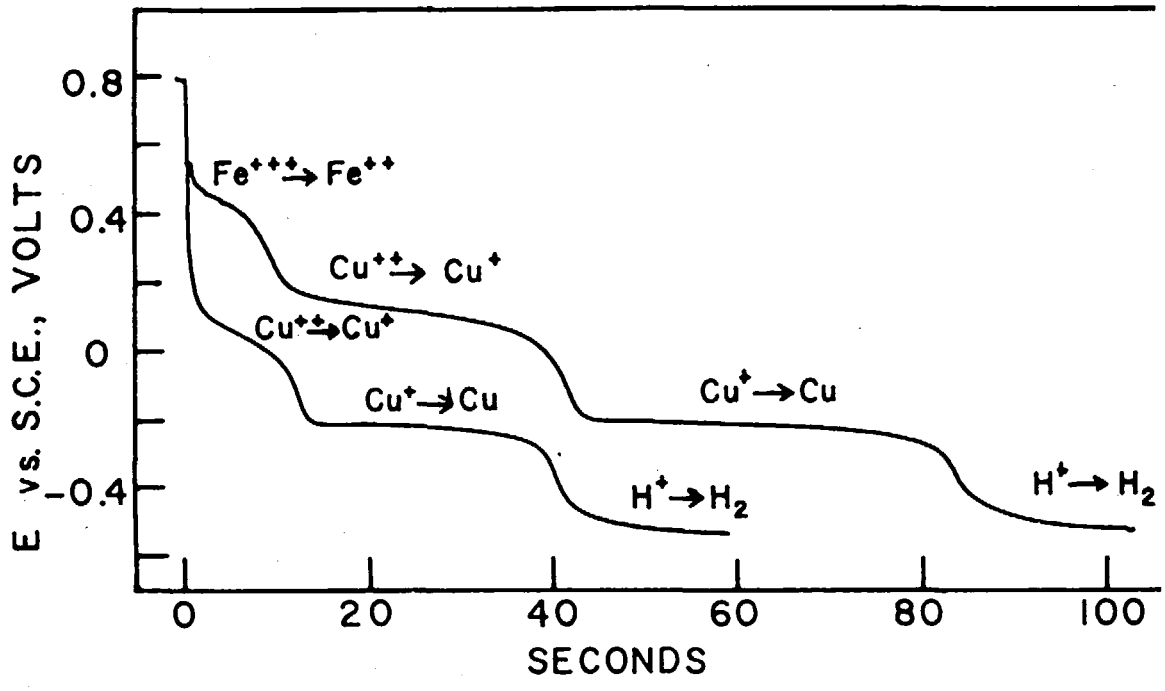

FIGURE 12. Chronopotentiograms for the reduction of 5 m*M* copper (II) and for a mixture of 5 mM copper (II) and 5 m*M* iron (III) in 1 *M* HCl. i_o = 830 μA/cm^2. From Ref. 1. With permission.

produced or consumed at the electrode, is given by[85,86]

$$\nabla Cu(I)\Big|_{x=0} = -2i_o/\pi FD \arcsin[2\tau/t-1];\ t \geq \tau \qquad (43)$$

where D is the diffusion coefficient of Cu(I). This equation predicts that the reactions immediately after the first transition time will be

$$Cu(II) + e \rightarrow Cu(I)$$
$$Cu(II) + 2e \rightarrow Cu(0)$$

Note that the reduction of Cu(I) to Cu(0) does not occur at this time. The fraction of the Cu(II) being reduced all the way to Cu(0) will increase with time after the first transition time to compensate for the continuing decrease in the flux of Cu(II) to the electrode. Until $t = 2\tau$, Cu(I) will continue to be produced in the solution and it is only at this point, when the flux of Cu(II) decreases to less than half its value before the transition time, that Cu(I) production ceases and the Cu(I) previously produced in the solution begins to move back to the electrode to be reduced. After $t = 2\tau$, the electrode reactions are

$$Cu(II) + 2e \rightarrow Cu(0)$$
$$Cu(I) + e \rightarrow Cu(0)$$

Evans[86] demonstrated the validity of these statements by following the production of hydrogen peroxide during the stepwise reduction of oxygen at a mercury cathode.

For a mixture, the length of the second and subsequent transition times is given by[61,85]

$$(\tau_1 + \tau_2 + \ldots + \tau_N)^{1/2} - (\tau_1 + \ldots + \tau_{N-1})^{1/2} = n_N F\sqrt{\pi D_N}\, C_N^*/2i_o \qquad (44)$$

where the parameters forming the right-hand side of this expression are characteristic of the Nth species and the transition time for the Nth species is measured from the transition time for the (N-1)th species. Thus, $\tau_1 + \tau_2 + \cdots + \tau_N$ represents the entire time interval of the experiment.

For the two-step reaction of a single substance, this equation reduces to

$$\tau_2/\tau_1 = 2n_2/n_1 + (n_2/n_1)^2 \qquad (45)$$

For the stepwise reduction of copper, $n_1 = n_2$ and so $\tau_2 = 3\tau_1$.

The ratio of successive transition times can become quite large. For example, one would predict a ratio of 35 for the stepwise oxidation of iodide to iodine and subsequently to iodate. This is close to what is observed.[87]

This enhancement of the second wave is of slight advantage analytically in the occasional circumstance that the component more difficult to reduce is at a much lower concentration. For example, if the Fe(III)/Cu(II) ratio were ten and one tried to determine the copper by controlled-potential electrolysis (at a platinum electrode!), he would be forced to make a 90% correction for the iron background. On the other hand, the ratio of the iron to copper transition times is more nearly five to one so that the background correction is less. However, the suggestion that one might deliberately add a more readily reduced component to enhance the transition time seems valueless since one could just as well lengthen the transition time by decreasing the current density.

VIII. CHRONOPOTENTIOMETRY WITH CURRENT REVERSAL

Let us suppose that at some time during a chronopotentiometric experiment before the transition time, i.e., $t_f \leq \tau$, one were to reverse the direction of current flow to cause the R produced during the initial portion of the experiment to be oxidized to O. If we are to determine the concentration profile during this reversal, we must solve the diffusion equation subject to the following initial and boundary conditions.

Initial Condition (Equation 19)

$$C_R(x,t_f) = \frac{2i_o}{nF}\sqrt{\frac{t_f}{\pi D_R}}\exp\left(\frac{-x^2}{4D_R t_f}\right) - \frac{i_o x}{nFD_R}\operatorname{erfc}\sqrt{\frac{x^2}{4D_R t_f}} \qquad (46)$$

(This assumes $C_R(x,0) = C^*_R = 0$. Cf. Equation 2.)

Boundary Conditions:

$$\lim_{x\to\infty} C_R(x,t) = 0$$

$$D_R \nabla C_R(0,t) = i_o'/nF; \quad t > t_f \qquad (47)$$

The solution is[85]

$$C_R(x,t') = \frac{2i_o}{nF}\sqrt{\frac{t_f+t'}{\pi D_R}}\exp\left(\frac{-x^2}{4D_R(t_f+t')}\right) - \frac{i_o x}{nFD_R}\operatorname{erfc}\sqrt{\frac{x^2}{4D_R(t_f+t')}} - \frac{2(i_o+i_o')}{nF}\sqrt{\frac{t'}{\pi D_R}}\exp\left(\frac{-x^2}{4D_R t'}\right) + \frac{(i_o+i_o')x}{nFD_R}\operatorname{erfc}\sqrt{\frac{x^2}{4D_R t'}} \qquad (48)$$

where $t' = t - t_f$

and i_o = current density before reversal

i_o' = current density after reversal

Both i_o and i_o' are positive.

The concentration profiles for R predicted by this equation are depicted in Figure 13. Note that after the reversal, R diffuses *both* to the electrode and away from it. The diffusion of R away from the electrode is clearly indicated by the fact the concentration of R at longer distances from the electrode ($\sim$ 0.004 cm in this example) actually *increases* after t_f, due to the continued diffusion of R away from the electrode.

At the reverse transition time, indicated as the time at which $C_R(0,t)$ goes to zero, the solution still contains considerable R. If the current densities for the forward and reverse are of equal magnitude, then the ratio of the reverse to forward times is a measure of the fraction of material reoxidized and this ratio must be less than one.

The transition time for the reverse process occurs when $C_R(0,\tau_r) = 0$. Consequently,

$$\tau_r = \frac{i_o^2 t_f}{(i_o+i_o')^2 - i_o^2}; \quad t_f < \tau \qquad (49)$$

When the current is exactly reversed, so that $i_o = i_o'$,

$$\tau_r = t_f/3 . \qquad (50)$$

Note that this widely quoted relationship is valid no matter how disparate the values of the diffusion coefficients of O and R. If the diffusion coefficient of R is particularly high, then the concentration profile for R will extend a long distance into the solution at the time of reversal. However, the larger diffusion coefficient means

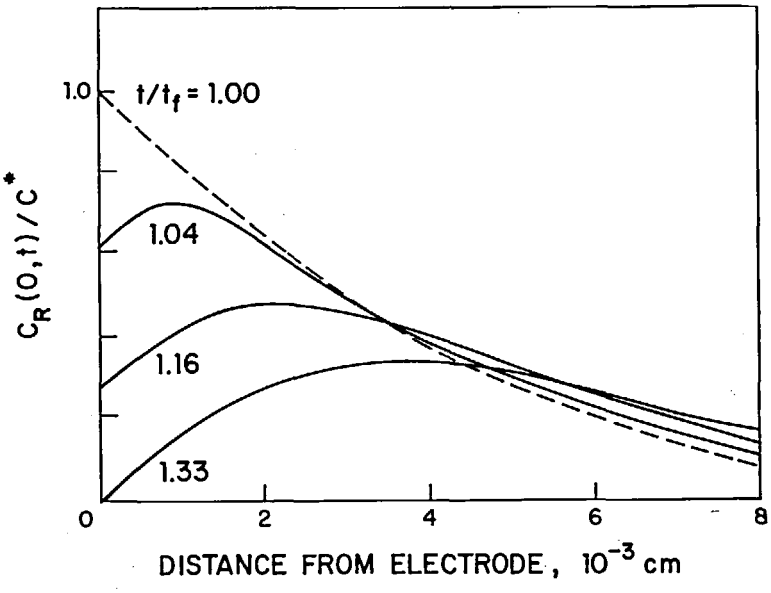

FIGURE 13. Concentration profiles of R as a function of time following current reversal. $D_R = 1 \times 10^{-5}$ cm²/sec. Adapted from Ref. 85. With permission.

that R will be able to diffuse more rapidly back to the electrode when the current is reversed.

The discussion so far has assumed that both species are soluble and stable in the solution. If the product of the electrode reaction is unstable, the ratio t_f/τ_r will be increased because the reverse time will be shortened. The exact value of this ratio will depend on the rate constant and on t_f, and by measuring the ratio as a function of t_f, it is possible to determine the value of the rate constant. If the product is insoluble (Cu(I) → Cu(0), for example) or adsorbed,[89, 114] then the reverse time will be lengthened; in the limit in which all the product is adsorbed, $t_f/\tau_r = 1$.

Experimental values of the ratio t_f/τ_r have been measured for current-reversal experiments in which the reverse current is less than the forward current and agreement with theory has been obtained.[89] For the reduction of cadmium ion, Cd^{++} → Cd(Hg), followed by oxidation of the cadmium amalgam, Cd(Hg) → Cd^{++}, and apparent forward electrolysis times (t_f)cn the order of several seconds, good agreement was found for values of the ratio t_f/τ_r from 3:1 to 1:2. Although one might guess that the precision and accuracy of this measurement would increase as the ratio of forward to reverse times approached unity, no such effect was observed.

The separation of the forward and reverse waves on the potential axis is often used as a quick test for reversibility. For example, for the interconversion of two soluble monomeric species ($D_O = D_R$), the potential-time curve upon current reversal should conform to Equation 51

$$E = E_{\frac{1}{2}} + \frac{RT}{nF} \ln \left[\frac{t_f^{\frac{1}{2}} - (t_f + t')^{\frac{1}{2}} + 2t'^{\frac{1}{2}}}{(t_f + t')^{\frac{1}{2}} - 2t'^{\frac{1}{2}}} \right] \quad (51)$$

so that $E = E_{1/2}$ when $t' = 0.215\tau_r$ for $t_f = \tau$. For the forward process, $E = E_{1/2}$ when $t = 0.250\tau$. Hence, any separation of the curves indicates irreversibility. This assumes of course that the electrode placement is such that the iR drop across the uncompensated resistance between the working electrode and the reference electrode is negligible.

It is not widely emphasized that the potential-time curve upon reversal intersects $E_{1/2}$ when $t = 0.215\ \tau_r$ only if the reversal takes place exactly at the forward transition time. If the reversal takes place before the forward transition time, the potential-time curve upon reversal will intersect $E_{1/2}$ *before* $t = 0.215\ \tau_r$. For example, for $t_f/\tau = 0.8$, 0.6, and 0.4, $E = E_{1/2}$ occurs at about $t/\tau_r = 0.164$, 0.104, and 0.035, respectively. Nonetheless, $E(0.25t_f)$ equals $E(0.215\tau_r)$ for a reversible couple although, in general, this potential is different from the half-wave potential. Of course, all these relationships fail if the stoichiometry is other than O + ne = R, where both O and R are soluble. For a totally irreversible process, the E-t curve following reversal should be given by

$$E = \frac{RT}{(1-\alpha)nF} \ln \frac{\sqrt{\pi D_R}}{2k_b} - \frac{RT}{(1-\alpha)nF} \ln[(t_f + t')^{\frac{1}{2}} - 2t'^{\frac{1}{2}}] \quad (52)$$

The case of a quasi-reversible system has been treated quite generally by Anderson and Macero.[90] Non-zero initial concentrations of product shift the entire chronopotentiometric wave along the potential axis but do not affect the shape of the waves nor the separation of forward and reverse waves. As one would expect, the separation of the forward and reverse waves on the potential axis increases with decreasing $k_{s,h}$. Changing α distorts the shape of the waves but the separation, measured as the difference between the 0.250-wave potential of the forward process and the 0.215-wave potential of the reverse process, is insensitive to the exact value of α when this has values in the range 0.3 to 0.7.[91] This last observation led Beyerlein and Nicholson[91] to propose the measurement of the difference in "quarter-wave potentials" as a rapid and simple way to evaluate electrode kinetics. This approach has not been widely applied, nor is it likely to be because the vagaries of measuring reverse-current transition times and the distortion of potential-time curves, due to double-layer charging[59] and other effects, are more severe than in ordinary forward chronopotentiometry. On this last point, decreasing the current density upon reversal may be advantageous because this will lengthen the reverse wave, thereby improving the resolution of the potential-time curve, and it will decrease the effect of double-layer charging, thereby lessening the distortion of the potential-time curve.

Here, too, one must be careful about where one reverses the current. The curves of Beyerlein and Nicholson[91] were calculated assuming reversal at

$t_f = \tau$. For reversal at other times less than τ, one should calculate new working curves. The difference between $E(0.25t_f)$ and $E(0.215\tau_r)$ is approximately constant over the range $0.4 < t_f/\tau < 1.0$ for $\alpha = 0.5$, but I would not expect such constancy for α-values much different from 0.5 (cf. Table 5).

TABLE 5

Separation of Quarter Wave Potertials for a Quasi-Reversible System as a Function of Time of Reversal. α = 0.5; ψ = 1.0.

$t_f/$	$E(0.25t_f)$*	$E(0.215\tau_r)$*	Δ E,mV
1.0	− 45.3	+ 45.1	90.4
0.8	− 40.0	50.8	90.8
0.6	− 34.5	58.0	92.5
0.4	− 28.2	67.7	95.9

*With respect to $E_{1/2}$

IX. CHRONOPOTENTIOMETRY IN THE ABSENCE OF SUPPORTING ELECTROLYTE

The modifications of the "diffusion equations" needed, in the absence of supporting electrolyte, to account for the transport of ionic species by "migration" have been fully discussed by Kies[92] and by Morris and Lingane.[93, 94] Fick's first law becomes

$$\vec{J} = -\frac{CD}{RT}\nabla\bar{\mu} = -D(\nabla C + \frac{zFC}{RT}\nabla\phi) \qquad (53)$$

where $\bar{J}$ and $\bar{\mu}$ are the flux density and the electrochemical potential of a particular ionic species and ϕ is the electrical potential in the solution. Fick's second law becomes

$$\frac{\partial C_j}{\partial t} = \nabla\cdot D_j(\nabla C_j + \frac{z_jFC_j}{RT}\nabla\phi);$$
$$j = 1, 2, \ldots N \qquad (54)$$

When an equation of this form is written for the electroactive species (j = 1) in the presence of excess supporting electrolyte, the product $z_1C_1\nabla\phi$ is negligible and the more familiar form of this law results. Cf. Equation 1.

It is usual to assume that the diffusion coefficient is independent of position in the solution, i.e., $\nabla D = 0$. Thus, Equation 54 becomes

$$\frac{\partial C_j}{\partial t} = D_j\nabla^2C_j + \frac{z_jFC_jD_j}{RT}\nabla^2\phi + \frac{z_jFD_j}{RT}\nabla C_j\cdot\nabla\phi;\ j = 1, 2, \ldots N \qquad (55)$$

In general, an equation of this form must be written for each species in the solution and the resulting system of simultaneous differential equations solved for the various solution concentrations.

Certain simplifications result if the solution contains only two *ionic* species as, for example, in the reduction Zn(II) + 2e → Zn(Hg). Under these conditions, there are only two equations of the form of Equation 55 and $n = z_1$.

$$\frac{\partial C_1}{\partial t} = D_1\nabla^2C_1 + \frac{z_1FC_1D_1}{RT}\nabla^2\phi + \frac{z_1FD_1}{RT}\nabla C_1\cdot\nabla\phi \qquad (56)$$

$$\frac{\partial C_3}{\partial t} = D_3\nabla^2C_3 + \frac{z_3FC_3D_3}{RT}\nabla^2\phi + \frac{z_3FD_3}{RT}\nabla C_3\cdot\nabla\phi \qquad (57)$$

where the subscript "1" denotes the electroactive species (i.e., Zn(II)) and the subscript "3" the counter ion. Using the electroneutrality expression $z_1C_1 + z_3C_3 = 0$†, we combine Equations 56 and 57 to obtain

$$\frac{\partial C_1}{\partial t} = D_s\nabla^2C_1 \qquad (58)$$

where

$$D_s = D_1D_3(z_1-z_3)/(z_1D_1-z_3D_3) \qquad (59)$$

Note that the *form* of Equation 58 is identical to the usual formulation of Fick's second law with a different proportionality factor.

The current passing through the cell is the sum

†The validity of this assumption has been discussed by Levich with an approximate diffusion layer treatment. Cf. V. G. Levich, *Physicochemical Hydrodynamics*, Prentice-Hall, Inc., Englewood Cliffs, N. J., 1962, 248.

of the charge flux densities of both the anions and the cations.

$$\frac{\vec{I}}{F} = -z_1 D_1 \left(\nabla C_1 + \frac{z_1 F}{RT} C_1 \nabla\phi\right) - z_3 D_3 \left(\nabla C_3 + \frac{z_3 F}{RT} C_3 \nabla\phi\right) \quad (60)$$

Since the flux of C_3 is zero at the electrode surface,

$$\left.\frac{\vec{I}}{F}\right|_{x=0} = \frac{i_o}{z_1 F} = D_1 \left(\nabla C_1 + \frac{z_1 F}{RT} C_1 \nabla\phi\right)\cdot\hat{x}\Big|_{x=0} \quad (61)$$

and

$$\nabla\phi\cdot\hat{x}\Big|_{x=0} = -\frac{RT}{z_3 F C_3} \nabla C_3\cdot\hat{x}\Big|_{x=0} \quad (62)$$

Therefore the current density at the electrode surface is given by

$$\frac{i_o}{z_1 F} = D_1 \frac{z_3 - z_1}{z_3} \nabla C_1\cdot\hat{x}\Big|_{x=0} \quad (63)$$

Thus, the *form* of the expression relating the current density and the concentration gradient of the reactant is unchanged in the absence of supporting electrolyte.

These basic equations define the mass transport problem in the absence of supporting electrolyte. Because the *form* of Fick's second law and the *form* of the boundary conditions are unchanged in the absence of supporting electrolyte, the *form* of the solutions for C_1 and C_3 is unchanged and the parametric dependences of these solutions on time, current density, bulk concentration, etc. are not altered. The transition time observed in the absence of supporting electrolyte should, therefore, be given by

$$i_o \tau^{1/2} / C^* = nF \sqrt{\pi D_s}/2(1-T_1) \quad (64)$$

where T_1 is the transference number of the electroactive species.

$$1 - T_1 = T_3 = z_3\lambda_3/(z_1\lambda_1 + z_3\lambda_3) \quad (65)$$

Morris and Lingane[93] demonstrated the accuracy of this expression for the reduction of thallous and cupric sulfates. By adding K_2SO_4, they were able to show that this expression, with more general definitions of D_s and T_1, is approximately valid at intermediate supporting electrolyte concentrations. As one would predict, the transition time for the reduction of benzoquinone, a non-electrolyte, was not enhanced upon removing supporting electrolyte.

X. CORRECTION FOR DOUBLE-LAYER CHARGING IN THE ABSENCE OF SUPPORTING ELECTROLYTE

Changes in the electronic charge density of the surface of an electrode are accompanied by changes in the ionic concentrations next to the electrode even in the absence of a faradaic electrode reaction. In dilute solutions of electrolytes, and especially in the absence of supporting electrolyte, these concentration perturbations are very appreciable and must be considered in the derivation of the relation for the transition time. The unexpected conclusion is that no charging corrections are to be applied in the absence of supporting electrolyte; the transition time to be employed in the modified Sand Equation is simply the total electrolysis time. The argument is straightforward. Anson writes[95]

$$i_o T_1^{dl}/z_1 F = D_1(\nabla C_1 + z_1 C_1 \nabla\phi)_{x=0} \quad (66)$$

$$i_o T_3^{dl}/z_3 F = D_3(\nabla C_3 + z_3 C_3 \nabla\phi)_{x=0} \quad (67)$$

where $T_1{}^{dl}$ and $T_3{}^{dl}$ are the effective cationic and anionic transference numbers at the boundary of the diffuse layer. $T_1{}^{dl}$ and $T_3{}^{dl}$ may be more formally defined as $\partial q + /\partial q_m$ and $\partial q - /\partial q_m$, respectively, and can be calculated directly from the Gouy-Chapman theory of the diffuse double layer.[96] For our purposes it is sufficient to note that $T_1{}^{dl}$ is essentially unity, and $T_3{}^{dl}$ essentially zero, when the electrode surface charge density is more negative than about -4μ coulombs cm^{-2}.[97] This corresponds to potentials more than about 0.2 V cathodic to the point of zero charge.[98] $T_1{}^{dl}$ becomes unity because the excess charge in the diffuse layer is almost entirely cationic under these conditions and, hence, must be unity.

If one assumes a *faradaic process* of the form $M^{z1} + z_1 e \rightarrow M^o$,

$$i_o/z_1 F = D_1(\nabla C_1 + z_1 C_1 \nabla\phi)_{x=0} \quad (68)$$

$$0 = D_3(\nabla C_3 + z_3 C_3 \nabla\phi)_{x=0} \qquad (69)$$

(The faradaic anionic flux is zero under these conditions since this species does not take part in the faradaic process.) Note that Equations 66 and 68 and Equations 67 and 69 are identical under conditions that $T_1^{dl} = 1$ and $T_3^{dl} = 0$.

Because the fluxes are independent of whether the constant current is consumed by a faradaic or non-faradaic process, it follows that the concentration versus distance profiles will also be independent of the exact mix of faradaic and non-faradaic processes. Consequently, Equation 70 will describe the concentration of the electroactive cation

$$C_1(0,t) = C_1^* - \frac{2i_o(1-T_1)}{z_1F}\sqrt{\frac{t}{\pi D_s}} \qquad (70)$$

at the surface of the diffuse layer. Note that time is measured from the beginning of electrolysis, i.e., without any double-layer correction. The chronopotentiometric constant will be given by Equation 64. T_1 is the cation transference number in the bulk of the solution.

The good agreement between experiment and Equation 64 found by Morris and Lingane[93] reflects the fact that *all* double-layer charging effects were negligible on the several second time scale of their experiments.

XI. POTENTIAL-TIME CURVES IN THE ABSENCE OF SUPPORTING ELECTROLYTE

It is impossible to measure the potential difference between the working electrode and the reference electrode in solutions of low conductivity because of the large and position-sensitive iR voltage developed between the tip of even a Luggin capillary and the surface of the working electrode and because of a liquid-junction potential produced by the electrolysis of the material in the vicinity of the electrode. Fortunately, under conditions of constant current, the only requirement is that the sum of these voltages remain approximately constant during the course of the experiment since only a knowledge of the *change* in the potential of the working electrode is necessary for the determination of the transition time.

The gradient of the electrical potential is composed of an ohmic and a liquid-junction term and can be obtained at any point in the solution by substituting the electroneutrality relationship into Equation 60 to obtain

$$\nabla\phi = \frac{RT}{FC_1(z_1D_1 - z_3D_3)}\left[\frac{i_o}{z_1F} - (D_1 - D_3)\nabla C_1\right] \qquad (71)$$

We can calculate the potential change during electrolysis by integrating this expression.

$$V(t) = \int \nabla\phi \cdot d\vec{x} = \frac{RT}{F(z_1D_1 - z_3D_3)}\left[\frac{i_o}{z_1F}\int \frac{d\vec{x}}{C_1} - (D_1 - D_3)\int \frac{\nabla C_1}{C_1}\cdot d\vec{x}\right] \qquad (72)$$

The change in this voltage is given by $\Delta V(t) = V(t) - V0$. Hence,

$$\Delta V(t) = \frac{RT}{F(z_1D_1 - z_3D_3)}\left[\frac{i_o}{z_1F}\int \frac{C_1^* - C_1}{C_1C_1^*}\,dx - (D_1 - D_3)\ln\frac{C_1^*}{C_1(0,t)}\right] \qquad (73)$$

where C^*_1 is the bulk concentration of the electroactive species.

At a distance greater than the thickness of the diffusion layer from the surface of the electrode, $C_1 \sim C^*_1$. Thus, the integrand in Equation 73 is essentially zero for $x > 20\sqrt{D_s t}$ and only a negligible error results if this value of the distance coordinate is introduced as the upper limit of integration. With this assumption and the introduction of $C_1(x,t)$, the final expression is

$$\Delta V(t/\tau) = \frac{RT}{F(z_1D_1 - z_3D_3)}\left[D_1\frac{z_3 - z_1}{z_3}\sqrt{\frac{\pi t}{\tau}}\,\psi + (D_1 - D_3)\ln\left(1 - \sqrt{\frac{t}{\tau}}\right)\right] \qquad (74)$$

where

$$\psi = \int_0^{10} \frac{e^{-y^2} - \pi^{1/2} y \operatorname{erfc} y}{\sqrt{\frac{\tau}{t}} - e^{-y^2} + \pi^{1/2} y \operatorname{erfc} y} \, dy$$

and $y = x/2\sqrt{D_s t}$

Since the change in the sum of the iR voltage and the liquid-junction potential is a function only of the ratio t/τ, the distortion of the chronopotentiometric potential-time curves by changes in this voltage is independent of the current density and the solution concentration. The theoretical distortion of the potential-time chronopotentiogram for the reversible and irreversible reduction of substances with diffusional parameters similar to those of zinc perchlorate is illustrated in Figure 14.

In the presence of some supporting electrolyte, the variation of the sum of the liquid-junction potential and the iR voltage cannot be calculated analytically. However, the effects should be much less pronounced and probably totally negligible in the presence of even small amounts of supporting

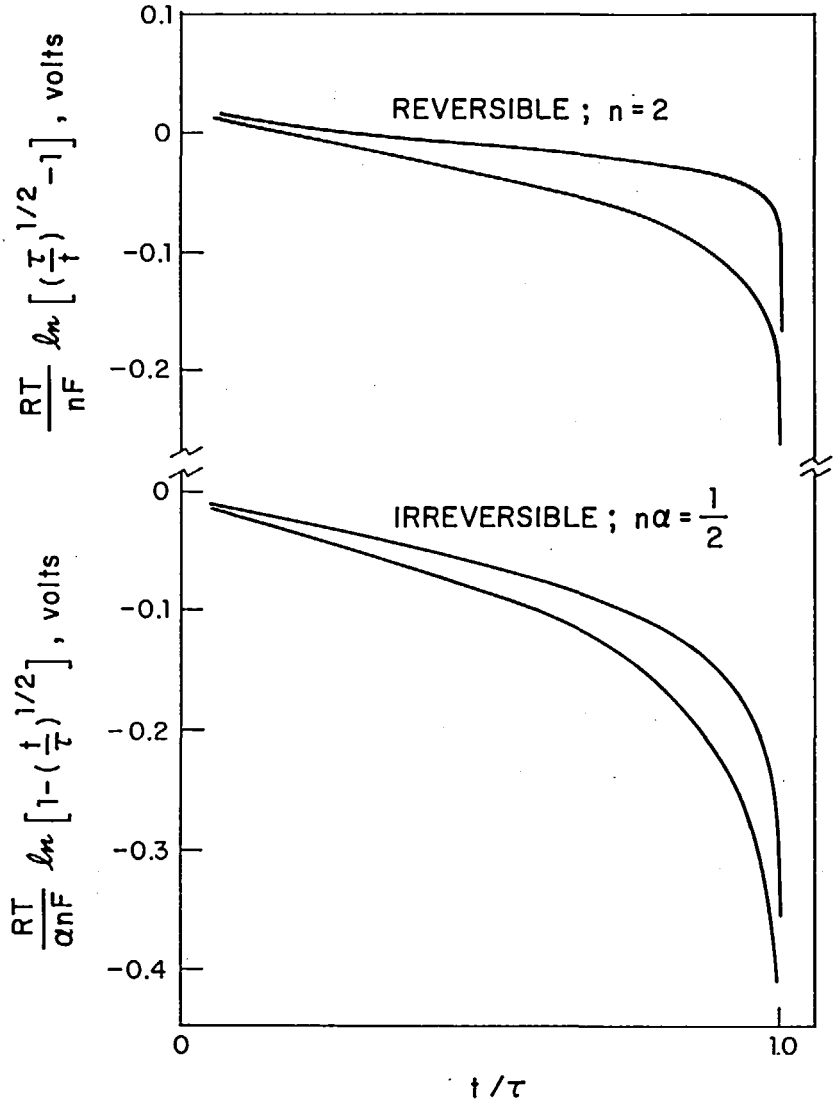

FIGURE 14. Schematic chronopotentiograms for the reversible and totally irreversible reduction of $Zn(ClO^{\Delta})_4$. The lower curve of each pair is the theoretical E-times curve to be observed in the absence of supporting electrolyte. Redrawn from Ref. 99.

electrolyte. In any event, the potential-time curves are still sufficiently well formed at reduced supporting electrolyte concentrations that transition times could be reasonably accurately determined.

In the absence of sufficient supporting electrolyte, doublet chronopotentiometric waves are observed for the reduction of solutions of chromate, cobalt(II), copper(II), thallium(I), and zinc(II) in water.[99, 100] The reduction of hydrogen ion produces only a singlet chronopotentiometric wave.[99] Figure 15 illustrates the effect of increasing current density on the morphology of the chronopotentiometric wave observed for the reduction of zinc chloride; the doublet character of the wave seems to disappear with increasing current density. These effects disappear completely in the presence of a tenfold excess of supporting electrolyte. Morris and Lingane[93] had investigated the chronopotentiometric reduction of both copper(II) and thallium(I) in the absence of supporting electrolyte at somewhat lower current densities than those employed here and only singlet waves are observed under their conditions.[99] No adequate explanation for these effects has been presented.

Experimental values of the chronopotentiometric constant observed[99] for the reduction of zinc(II) appear in Figure 16 as a function of the square root of the observed transition times. Data for the reduction of Co(II), Tl(I), and hydrogen ion are similar.[99] The transition times appropriate to the singlet chronopotentiometric waves were measured by the method of Reinmuth.[6] The transition time appropriate to two successive chronopotentiometric waves is normally taken to be the sum of the transition times of the individual waves and the total transition time appropriate to the doublet waves has been approximated in this fashion.[99] Since the experimental determination of chronopotentiometric transition times, even at moderate current densities, in the presence of excess supporting electrolyte and in the absence of multiple waves, is at best a consistent art, these data are open to ready criticism. The possibly controversial aspects of the procedures employed in these experiments were constantly and carefully considered during the analysis of these data and the qualitative aspects of these data are retained even if another procedure is adopted for the determination of the transition time.

The explanation for the decrease in the measured chronopotentiometric constant with increasing current density observed in the absence of supporting electrolyte is by no means complete. Part of the decrease can be ascribed to the method of transition-time measurement, i.e., a correction was applied (probably incorrectly, *vide supra*) for the initial double-layer charging. However, even if the transition time is measured from the start of electrolysis, $i_0\tau^{1/2}$ decreases at high current densities.[101] Part of the decrease might also be ascribed to the distortion of the potential-time curve due to the changing iR and liquid-junction potentials during electrolysis which has the effect

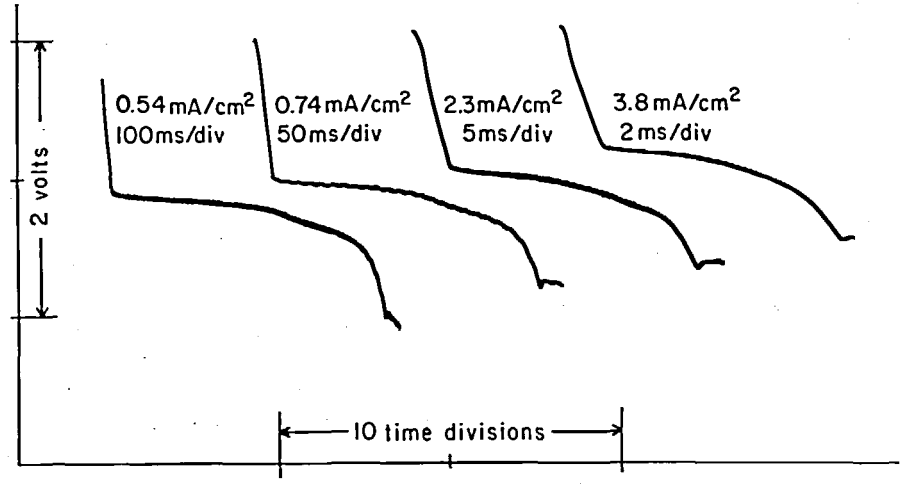

FIGURE 15. Experimental chronopotentiograms observed for the reduction of 0.4 m*F* $ZnCl_2$, pH = 6.7, in the absence of supporting electrolyte. The absolute potential scale is unknown (because of iR_u); the curves were shifted upwards form one another with increasing current density solely to aid in the clarity of the presentation. From Ref. 99.

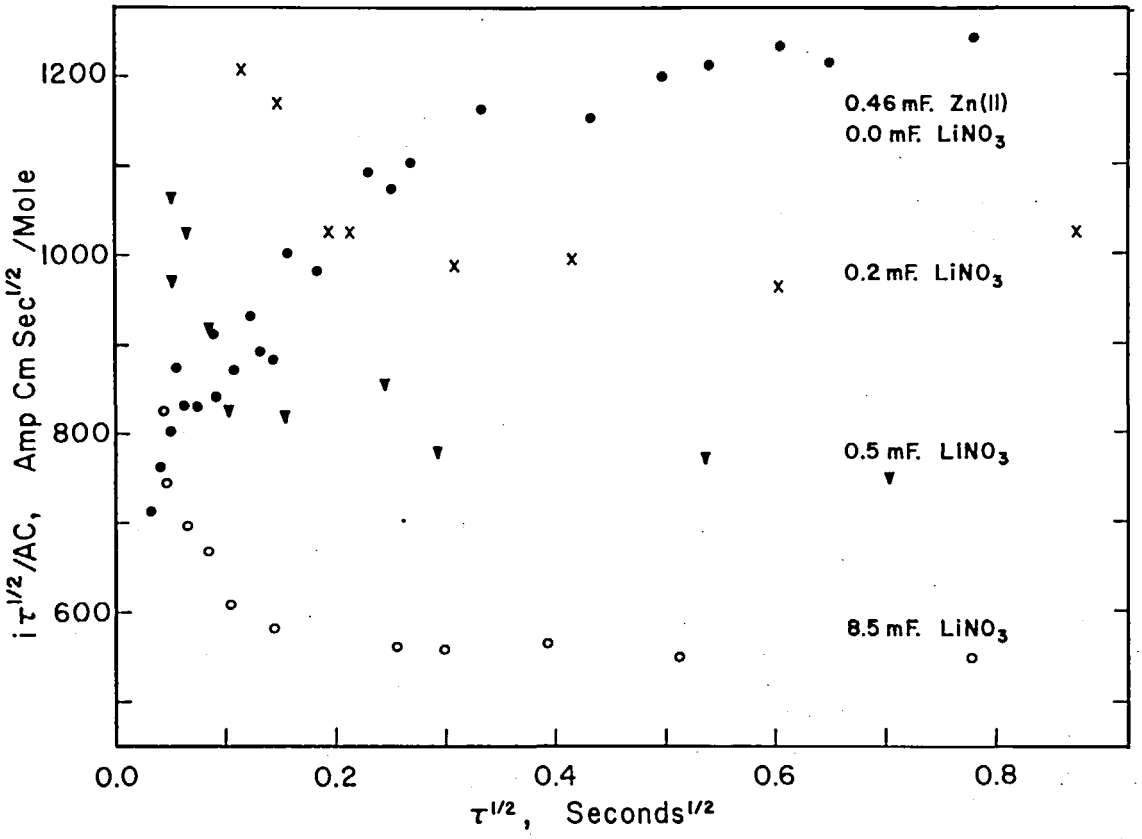

FIGURE 16. Chronopotentiometric constant as a function of $\tau^{1/2}$ for the reduction of zinc(II) in the presence of increasing amounts of supporting electrolyte. pH ~5.5. From Ref. 99.

of decreasing the slope of the potential-time trace in the vicinity of the transition time and thereby shortening transition time values measured by graphical techniques. Nevertheless, even if the transition time is measured at a point well after the inflection point, the $i_0\tau^{1/2}$ values are still too small at high current densities.[101]

Other possibilities include a slow chemical process preceding the electron-transfer step, a process whose rate increases markedly with ionic strength, or an explanation which calls into question the very meaning of a transition time in solutions containing no supporting electrolyte.

The explanation for the increase in $i_0\tau^{1/2}$ observed in these systems when small amounts of electrolyte are present is no more certain. One possibility, and in fact it was to test this that the experiments were performed originally, is that the diffuse layer is initially composed largely of electroactive ions† but that at the transition time these have been replaced by cations from the supporting electrolyte. This release of electroactive material close to the electrode is qualitatively similar to the reaction of adsorbed material and should lead to an increase of $i_0\tau^{1/2}$ at high current densities. There are several qualitative difficulties with this explanation, however. In particular, the transition times at high current densities should depend on the potential at which the electrode is initially biased, becoming longer the more negative the initial potential because of the increase in positive charge of the diffuse layer as the potential is made more negative. Yet the observed transition time values would appear to be independent of the initial potential. Furthermore, the amounts of released electroactive material calculated on the basis of the "constant current efficiency" model are much too large to be compatible with the Gouy-Chapman model of the diffuse layer.[99]

†If the potential is more negative than that at the point of zero charge, if the electroactive species is a cation, and if the charge of the electroactive species is greater than that of the cation of the supporting electrolyte.[99,102]

XII. MEASUREMENT OF ELECTRODE KINETICS

Previous reference has been made to the determination of the parameters of the electron-transfer step by analysis of the shape of the chronopotentiometric potential-time curve. In this section, a general method of data analysis and the influence of double-layer charging on the estimates of the parameters will be discussed. It will be assumed that the chronopotentiometric potential-time curve is described by Equation 75.[9, 90, 91] (This equation appeared earlier, in a different form, as Equation 22.)

$$H(E_i,t_i,\tau,\alpha,k_{s,h}) = \sqrt{t_i/\tau}\,(1+\exp[G(E_i)]) + \psi\exp[\alpha G(E_i)] - 1 = 0 \qquad (75)$$

where

$$G(E_i) = nF(E_i-E_{1/2})/RT$$

$$\psi = \frac{i_o(D_O/D_R)^{\alpha/2}}{nFC^*k_{s,h}} = \frac{\sqrt{\pi D_O}(D_O/D_R)^{\alpha}}{2k_{s,h}\tau^{1/2}}$$

$$E_{1/2} = E^{o\prime} + \frac{RT}{2nF}\ln D_R/D_O \qquad (76)$$

and the other symbols have their usual significance. The assumptions inherent in Equation 75 are the usual ones: that the heterogeneous electron-transfer processes are of first order; that the sum of the transfer coefficients appropriate to the anodic and cathodic processes is unity; that both the oxidized and reduced species are soluble and stable in the solution; and that diffusion is the only mass transport process. Potential-time curves appropriate to other stoichiometries have been derived.[9,103]

The dimensionless parameter ψ, used here to characterize the rate of the electron-transfer process, should be distinguished from the parameter ψ_{dl} used previously to gauge the degree of distortion of the potential-time curve by double-layer charging processes.

For fast electron-transfer processes, i.e., for small ψ, Equation 75 reduces to the expression for a reversible chronopotentiometric wave, Equation 23. For slow processes, i.e., large ψ, Equation 25 predicts that a plot of $(E-E_{1/2})$ vs. $\log [1 - \sqrt{t/\tau}]$ should be linear with a slope of $2.3RT/\alpha nF$ and an intercept value of $(2.3RT/\alpha nF) \log [nFC^*k_{s,h}/i_o]$, from which the parameters of the electron transfer process can be calculated.

In order to define "small ψ" and "large ψ" more precisely, Figure 17 shows a plot, as a function of ψ, of the error which results in $\sqrt{t/\tau}$ when one of the limiting expressions is used in place of Equation 75. If one is to determine the kinetic parameters, it is clear from this plot that the experimental conditions must be chosen such that ψ is at least 0.03; $\psi > 0.1$, where the error is about 9%, is perhaps more realistic. At $\psi = 0.1$ ($\alpha = 0.5$), the quarter-wave potential has shifted only 5 mV from $E_{1/2}$; the separation of forward and reverse "quarter wave potentials" is about 10 mV. The exact point where the totally irreversible expression becomes valid depends on the value of α but $\psi \simeq 10$ is a safe estimate.

These statements can be translated into more concrete terms by noting that ψ depends inversely on the *product* of the heterogeneous rate constant $k_{s,h}$ and the square root of the transition time. Thus, one can, in principle, transit from a completely reversible to a completely irreversible wave simply by decreasing the transition time of the experiment. However, there is a very practical lower limit to the transition time and, thus, an upper limit to the rates that can be measured chronopotentiometrically; this is set by the onset of distortion of the potential-time curve at ψ_{dl}-values much above 0.001. If we take ordinary values for the diffusion coefficient and double-layer capacity, 0.8×10^{-5} cm^2 sec^{-1} and 20 μF cm^{-2}, respectively, the transition time must, therefore, fall in the range

$$2 \times 10^{-6}/n^2C^* < \tau^{1/2} < 0.025/k_{s,h}$$

Consequently, the absolute upper limit for measureable values of $k_{s,h}$ is about 0.01 cm sec^{-1} for $n^2C^* = 10^{-6}$ equivalents cm^{-3} and about 0.1 cm sec^{-1} for $n^2C^* = 10^{-5}$ equivalents cm^{-3}. Rates ten times slower than this are probably about the practical upper limit for determination by the chronopotentiometric technique.

The $\psi > 10$ criterion for a totally irreversible chronopotentiometric process is equivalent to $\tau^{1/2} < 2.5 \times 10^{-4}/k_{s,h}$. Combining this with the further restriction that $\psi_{dl} < 0.001$, we obtain the following range of transition-time values for a totally irreversible wave.

$$2 \times 10^{-6}/n^2C^* < \tau^{1/2} < 2.5 \times 10^{-3}/k_{s,h}$$

For $n^2C^* = 10^{-6}$ equivalents /cm^3, the upper limit on $k_{s,h}$ is 1.3×10^{-4} cm/sec for a totally irreversible process.

It should be emphasized that a "linear log plot" is not a reliable criterion for a totally reversible or totally irreversible electrode reaction. To illustrate this, data were synthesized for $\alpha = 0.5$ as a function of ψ and were plotted according to both limiting expressions. The totally irreversible plots are shown in Figure 18. Note that apparent linearity is obtained with the totally irreversible expression even at ψ values well below the point at which the totally irreversible expression becomes valid but that the slope is decreased substantially from the correct value. Thus, the values of α derived from these plots are too large. Had one been sufficiently unfortunate as to use the limiting expression over a narrow range of ψ values in this "quasi-reversible" region, it is clear that considerable error would result in the estimates of $k_{s,h}$ and α.

Simple graphical techniques are not applicable for the estimation of kinetic parameters in the quasi-reversible region ($0.1 < \psi < 10$) where the totally irreversible expression (Equation 25) is inaccurate. However, this does not mean that one should avoid data in this region. On the contrary, data in this region can, in principle at least, be used to evaluate the standard potential of the couple,[90] thereby avoiding the need for an independent estimate of it.

The most satisfactory approach to the estimation of kinetic parameters from data taken in the quas-reversible region, or the totally irreversible region for that matter, is to adjust the data using Gaussian nonlinear least-squares techniques.[104-106] Very briefly, this approach involves defining a parameter h_i which is simply Equation 75 evaluated at the ith experimental data point using estimated values for α and for $k_{s,h}$. The best values of α and $k_{s,h}$ are taken to be those which minimize the sum $\Sigma w_i h_i^2$. w_i is a weighting function, taken in this instance to be

$$w_i = \left[\left(\frac{\partial H}{\partial E_i} \right)^2 \sigma_{E_i}^2 + \left(\frac{\partial H}{\partial t_i} \right)^2 \sigma_{t_i}^2 + \left(\frac{\partial H}{\partial \tau} \right)^2 \sigma_\tau^2 \right]^{-1} \qquad (77)$$

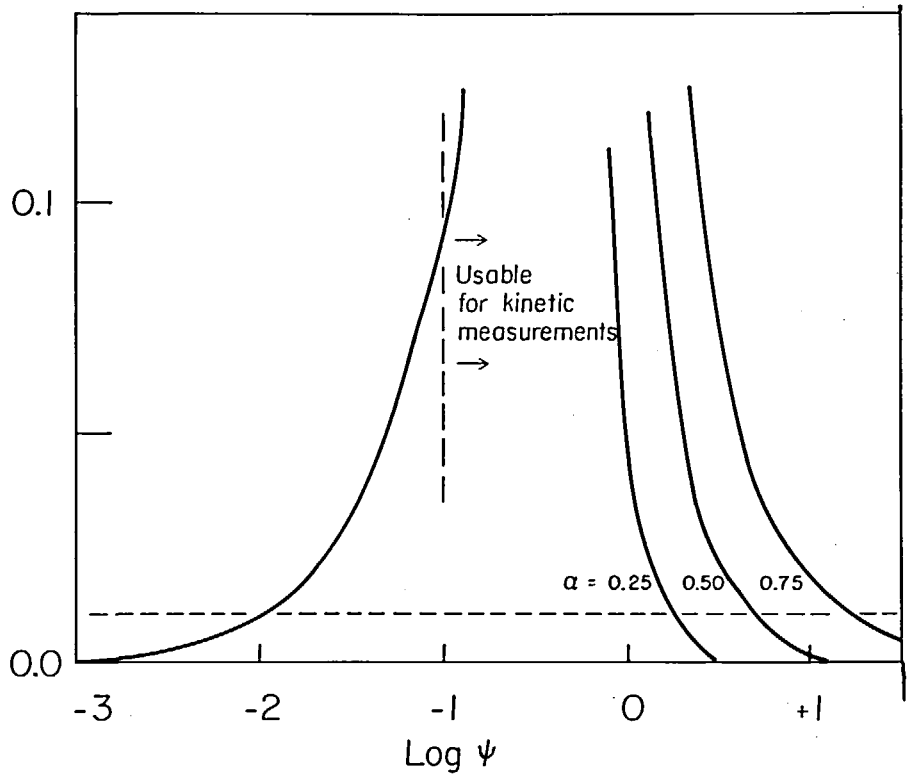

FIGURE 17. Error in $\sqrt{t/\tau}$ as a function of ψ.

This is an approximation since it ignores the fact that the errors at different data points are correlated because the error in a particular transition time measurement is common to several (E_i,t_i) values.[107]

Corrections to the initial estimates of α and of $k_{s,h}$ are calculated from the following matrix of normal equations.

$$\begin{bmatrix} \Sigma w H_\alpha H_\alpha & \Sigma w H_\alpha H_k \\ \Sigma w H_k H_\alpha & \Sigma w H_k H_k \end{bmatrix} \begin{bmatrix} \Delta \alpha \\ \Delta k \end{bmatrix} = \begin{bmatrix} \Sigma w H_\alpha h \\ \Sigma w H_k h \end{bmatrix} \quad (78)$$

where H_α and H_k denote differentiation with respect to α and $k_{s,h}$ respectively. Because H is a highly nonlinear function of α and $k_{s,h}$, one must iterate to achieve a final solution.

Anderson and Macero[90] have previously suggested an iterative technique for the treatment of chronopotentiometric data of intermediate reversibility. I feel most vigorously that their approach is not to be recommended because their treatment ignores the weighting function w. While this may appear to be of minor importance, it should be noted that the value of the weighting function varies by a factor of more than ten along a typical chronopotentiometric wave. If the weighting function is ignored, it can affect the accuracy of the results and, in any event, precludes the estimation of correlation coefficients, standard errors on the estimates of the parameters, and goodness-of-fit criteria.

Secondly, their approach is basically a trial-and-error method and is doubtless very inefficient. In our own experience fitting molar absorptivities and formation constants to spectrophotometric data, we have observed Gaussian techniques to be orders of magnitude more efficient than sophisti-

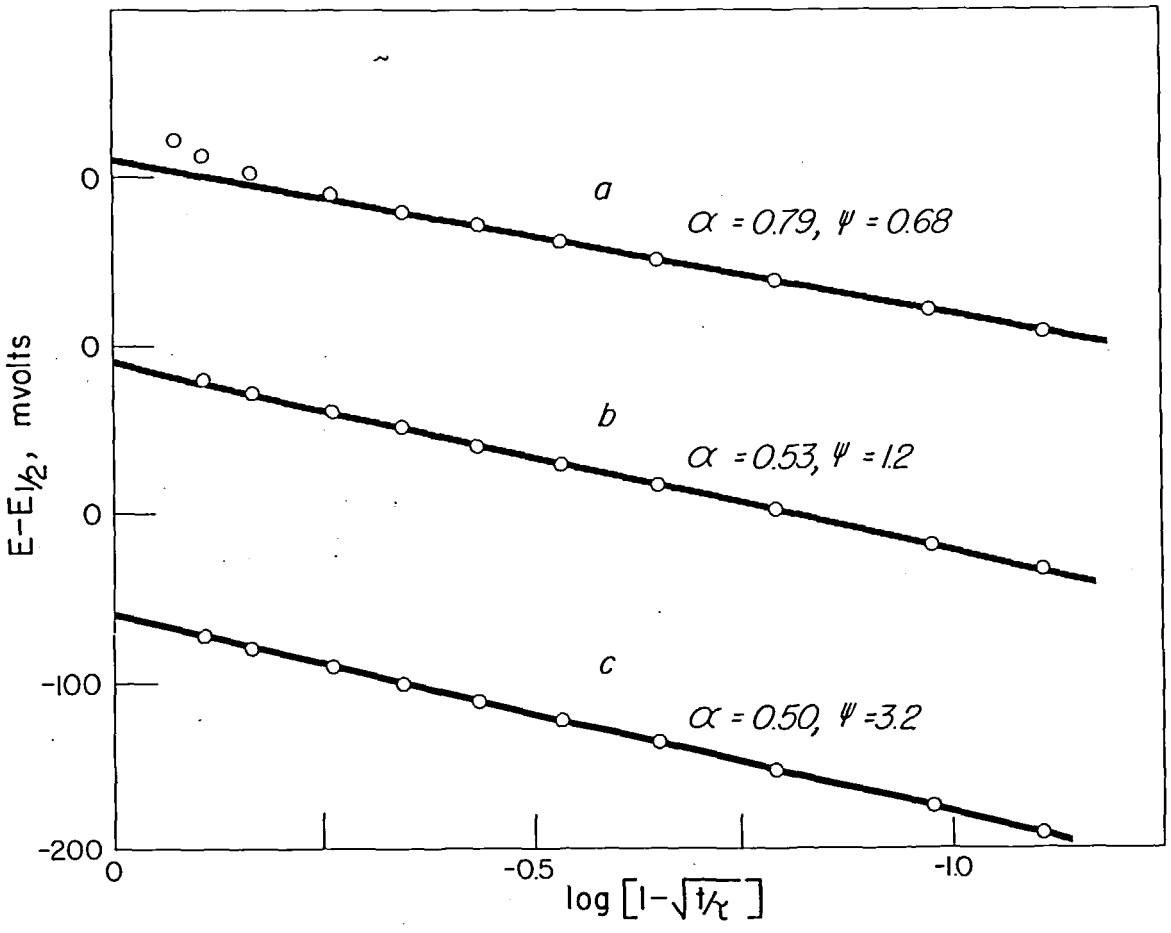

FIGURE 18. E-t data for a quasi reversible couple plotted according to the totally irreversible limiting expression, Equation 25. From Ref. 109.

cated numerical methods. This is a general observation.[108]

It is axiomatic that a properly weighted least-squares formalism will yield the same estimates of the parameters with a similar degree of precision for different formulations of the function H. The observation of Anderson and Macero,[90] to the effect that one formulation of H was superior for the estimation of $k_{s,h}$ and another was superior for the estimation of α, may well stem from their neglect of the weighting function.

Our experience with the least-squares estimation of the kinetic parameters has been with only one system, the Cu(II) + e = Cu(I) reaction at platinum in acetonitrile,[104] so that generalization is tenuous. However, it would appear that the iteration proceeds rapidly and smoothly to the correct parameters with a minimum likelihood of diverging or of ending up in a local minimum.

In principle, especially if one obtains data over a range of ψ values, one should be able to determine $E_{1/2}$ from the data.[90] The measured potentials are expected to be offset from the true potentials by an amount Ru where Ru is the uncompensated resistance between the working electrode and the reference electrode.[110] Again, in principle, one should be able to determine Ru from the data by covering a range of current densities. To do this, the normal equations matrix is expanded to include a total of four rows and four columns.[105,106]

It was our experience[109] that the iterative procedure did not refine when all four parameters were adjusted simultaneously. Therefore, α and $k_{s,h}$ were calculated as a function of a range of values of $E_{1/2}$ and Ru hoping that χ^2, the goodness-of-fit parameter, would vary sufficiently to permit the estimation of the optimum values for $E_{1/2}$ and Ru.

Unfortunately, the quality of the fit was not sensitive to the value of $E_{1/2}$. Apparently, these chronopotentiograms were sufficiently irreversible that a different value of the standard potential does not change the values calculated for α and, thus, would not change the internal consistency of the data; it does, of course, change $k_{s,h}$, but uniformly. The values of ψ ranged from about 0.6 to 3.

More significantly, the quality of the fit was not sensitive to the exact value chosen for the uncompensated resistance. This was especially disappointing because an independent determination of Ru is difficult. Decreasing the value chosen for the uncompensated resistance, which had the effect of moving the curves to more cathodic potentials, did not lead to different values of α. Apparently this is again because the curves were essentially totally irreversible. But the values of $k_{s,h}$ were not decreased uniformly since the iRu shifts in the data were not uniform. Increasing Ru shifted the waves anodic and both α and $k_{s,h}$ were now affected since the waves become quasi-reversible. Again, the effects were not uniform and the internal consistency of the data was lost, but the errors in (E_i, t_i) were apparently large enough that the value of χ^2 was not altered significantly.

The estimated values of α and $k_{s,h}$ are very strongly correlated in chronopotentiometry. That is, the least-squares minimum in the α, $k_{s,h}$ plane is a very shallow one and both α and $k_{s,h}$ can be offset from their correct values with very little change in the quality of the fit of the data. For example, the observed variables in the analysis of a totally irreversible wave are the slope and the intercept in a plot of $(E-E_{1/2})$ vs. $\log(1-\sqrt{t/\tau})$. To a first approximation, these two observations are independent. From the slope one can calculate α but the intercept depends on both α and $k_{s,h}$. Thus, the independent variables in this data analysis are *not* α and $k_{s,h}$ but rather α and $(k_{s,h})^{1/\alpha}$. Therefore, α and $k_{s,h}$ are correlated.

One promising way to avoid the effects of this correlation is to measure the difference in the "quarter-wave potentials" for a forward and reverse chronopotentiogram. Beyerlein and Nicholson[91] have observed that this difference is insensitive to the value of the transfer coefficient α when the transition time is such that the chronopotentiogram is quasi-reversible. Since the determination of $k_{s,h}$ under these conditions *does not* require a prior determination of either α or $E_{1/2}$, any error in α or $E_{1/2}$ is not propagated into an error in $k_{s,h}$.

Unfortunately, the Beyerlein and Nicholson[91] technique is applicable to a limited range of rate constants. It is not applicable to the faster electron-transfer processes where the reverse wave in particular is distorted by double-layer charging. Nor can it be applied to the very slow processes since it is not experimentally feasible to go to the very long times needed for quasi-reversibility.

Since Rodgers and Meites[57] have published theoretical E-t curves for a totally irreversible wave distorted by double-layer charging, it is possible to estimate the effect of double-layer charging on the

values of α and $k_{s,h}$ derived from these curves. We[109] have plotted their data according to the limiting irreversible expression; the curves are all apparently linear even with rather large values of the double-layer distortion parameter ψ_{dl}. The data appear in Figures 19 and 20. Note, however, that the α-values calculated from the slopes of these lines decrease from 0.5 for ψ_{dl}-values greater than about 0.001 and that the distortion is less marked in the case where the transition times were determined by the method of Reinmuth (Figure 19). The intercept ($t/\tau = 0$) values are constant at 0 ± 4 mV so that the apparent value of $k_{s,h}$, calculated from the ratio of slope to intercept, must be increasing with increasing ψ_{dl}. The empirical interrelationship may be expressed as follows:

$$(\alpha_{act}/\alpha_{obs}) \ln k_{obs} - \ln k_{act} = (1-\alpha_{act}/\alpha_{obs}) \ln[4RTC_{dl}/(nF)^2 \pi DC^* \psi_{dl}] \quad (79)$$

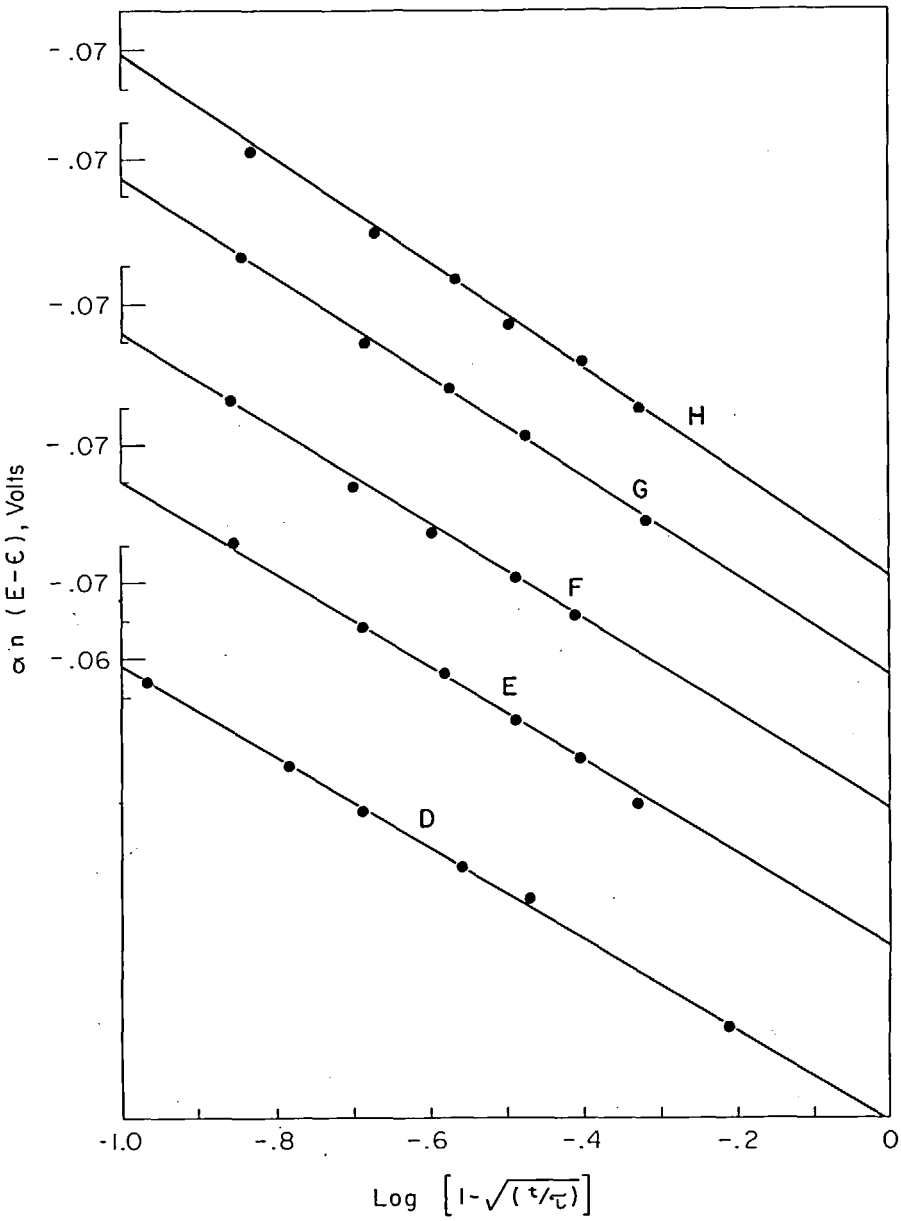

FIGURE 19. Effect on the transfer coefficient α of distortion of E-t curve due to double-layer charging (Reinmuth τ). From Ref. 109. ψ_{dl} and apparent α values are, respectively: D. 0.0006, 0.50; E. 0.0012, 0.49; F. 0.0024, 0.47; G. 0.006, 0.45; H. 0.012, 0.43.

The qualitative characteristic of this expression is that the ratio of the apparent rate to the true rate is larger the smaller the ratio C_{dl}/C and the smaller the absolute value of $k_{s,h}$.

In summary, it would seem that chronopotentiometry is ill suited to the determination of accurate kinetic parameters of rapid electron-transfer processes because of the distortion of the potential-time curves by double-layer charging.

XIII. CHRONOPOTENTIOMETRY AT A ROTATING DISC ELECTRODE

Buck and Keller,[111] several years ago, attempted to perform chronopotentiometry with a rotating disc electrode. It was shown both theoretically and experimentally that the chronopotentiometric constant, $i_o\tau^{1/2}/C^*$, for low applied currents, increases with increasing rotational speed. Under

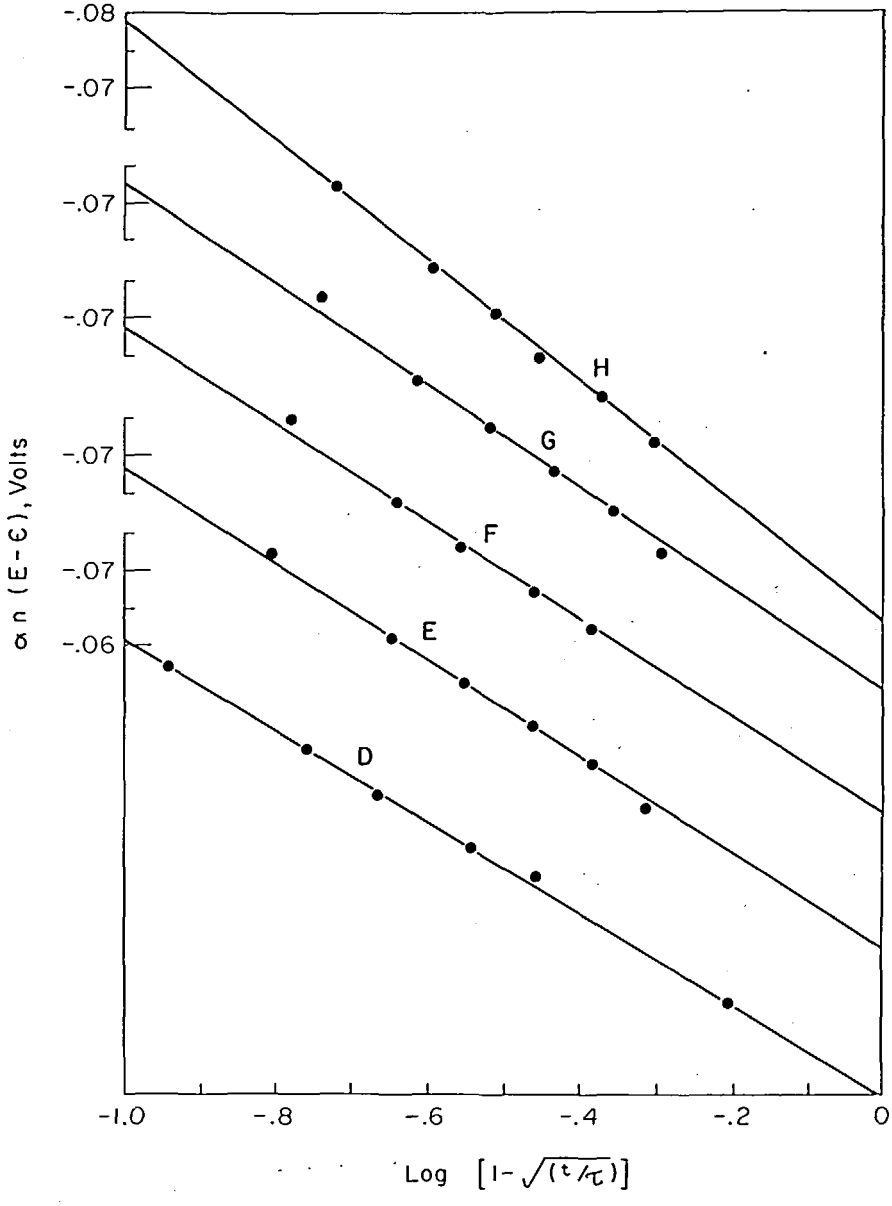

FIGURE 20. Effect on the transfer coefficient α of distortion of E-t curve due to double-layer charging (Kuwana τ). From Ref. 109. ψ_{dl} and apparent α values are, respectively: D. 0.006, 0.49; E. 0.0012, 0.46; F. 0.0024, 0.45; G. 0.006, 0.44; H. 0.012, 0.36.

these conditions, the diffusion layer thickness ($\sim\sqrt{Dt}$) is comparable to the Levich thickness ($D^{1/3}\nu^{1/6}/0.62\,\omega^{1/2}$) so that the rate of transport to the electrode is governed by both the rate of diffusion in the stationary boundary layer and by the mass-transport processes (stirring) caused by the rotation of the electrode. Since the latter increases with stirring rate, the overall transport to the electrode increases with rotation rate and thus $i_o\tau^{1/2}/C^*$ increases with rotation rate. On the other hand, if the current density is high, the transition time will be so short that the diffusion-layer thickness will be much smaller than the boundary layer. This condition is also achieved at low rotational speeds. Under these conditions, the Sand Equation is applicable and $i_o\tau^{1/2}/C^*$ is independent of rotational speed over that range where the diffusion-layer thickness remains much less than the Levich thickness.

The data of Buck and Keller[111] generally substantiated this argument although the precision of their data was rather poor. This technique would appear to offer no advantage over conventional chronopotentiometry, especially since one still has to worry about the distortion of the waves and the enhancement of the transition time by double-layer charging.

Hsueh and Newman[112] and, more recently, Miller and Bruckenstein[113] have proposed a constant-current rotating disc technique in which the potential of the disc is plotted against rotational speed. Such a technique is not, strictly speaking, chronopotentiometry since one does not record the disc potential as a function of time: Miller and Bruckenstein[113] suggest it be called "hydrodynamic potentiometry." Because this technique involves measurements under steady-state conditions, one is immediately freed from the effects of double-layer charging, a major advantage.

The form of the potential $\omega^{1/2}$ relations can be deduced most readily by reference to the current-potential relationship at constant rotational speed. As shown in Figure 21B, the current-potential curve for the reversible interconversion of two soluble species is of the familiar form of the polarographic wave viz.,

$$E = E_{1/2} - \frac{RT}{nF} \ln \frac{i}{i_\ell - i} \qquad (80)$$

where i_ℓ represents the limiting current density and is given by

$$i_\ell = 0.62\, nFC^* D^{2/3} \omega^{1/2} / \nu^{1/6} \qquad (81)$$

where ω is the rotational velocity in radians per second and ν is the kinematic viscosity.

If one operates at constant current and very high rotational velocity, the disc potential will fall somewhere on the rising portion of the current potential curve. The disc potential will not shift rapidly with changing rotational velocity because the current rises so rapidly in this region that the potential changes but slightly with the ratio of i/i_ℓ. However, when the rotational speed becomes so low that the ratio of constant current to limiting current approaches one, the potential will shift increasingly rapidly with further decreases in rotational speed. When the rotational speed decreases to the point where the constant current is equal to or larger than the limiting current, the potential of the disc will shift abruptly until stabilized by a second reaction. This potential $-\omega^{1/2}$ curve will be independent of double-layer charging effects.

At the critical rotational velocity, the impressed constant current exactly equals the limiting current so that for analytical purposes

$$i_o/\omega_c^{1/2} C^* = 0.62\, nFD^{2/3}\nu^{1/6} \qquad (82)$$

The form of the potential $-\omega^{1/2}$ curve for the reversible interconversion of two soluble species is derived by combining Equations 80 and 81

$$E = E_{1/2} - \frac{RT}{nF} \ln i_o + \frac{RT}{nF} \ln \left[(\omega/\omega_c)^{1/2} - 1\right] \qquad (83)$$

where ω_c is defined by Equation 82.

One must not be misled into thinking that the potential $-\omega^{1/2}$ curves will always be as well defined as shown here. If the limiting current region of the current potential curve is poorly defined because of a very irreversible electron-transfer process or because of overlapping electrochemical processes, the corresponding potential $-\omega^{1/2}$ curve will also be ill formed.

It is appropriate to compare this technique with the more conventional "hydrodynamic potentiometry",[113] i.e., current-potential curves, at a rotating disc electrode. One slight advantage is that it is usually easier to control the current through the cell constant than to maintain the potential difference between the working and reference electrodes constant. However, the penalty one pays is that the rotator must be capable of a continuous spectrum of rotational velocities

whereas, in the more conventional rotating disc experiment, a series of discrete rotational speeds, perhaps effected by a single synchronous motor and a series of gears, is all that is necessary.

The principal advantage of "hydrodynamic potentiometry" is likely to be realized in those situations where the uncompensated resistance is high, either because one has no or little supporting electrolyte[113] or because of the low dielectric constant of the solvent. This advantage belongs to all constant-current techniques.

As already stated, the advantage of this technique over conventional chronopotentiometry is that it is possible to eliminate the effects of double-layer charging by scanning the potential $-\omega^{1/2}$ curve slowly.

XIV. KINETIC PROCESSES: PRECEDING CHEMICAL REACTIONS

Some of the more significant possible applications of chronopotentiometry are to the study of systems in which chemical reactions precede, follow, or are in parallel with the electron-transfer processes. This discussion will only outline this area since kinetic applications of chronopotentiometry are being reviewed in depth.[116]

As the first example, we will assume that the electron transfer is preceded by a chemical reaction where the species Y is not oxidized or reduced.

$$Y \underset{k_b}{\overset{k_f}{\rightleftharpoons}} O + ne \rightarrow R \qquad (85)$$

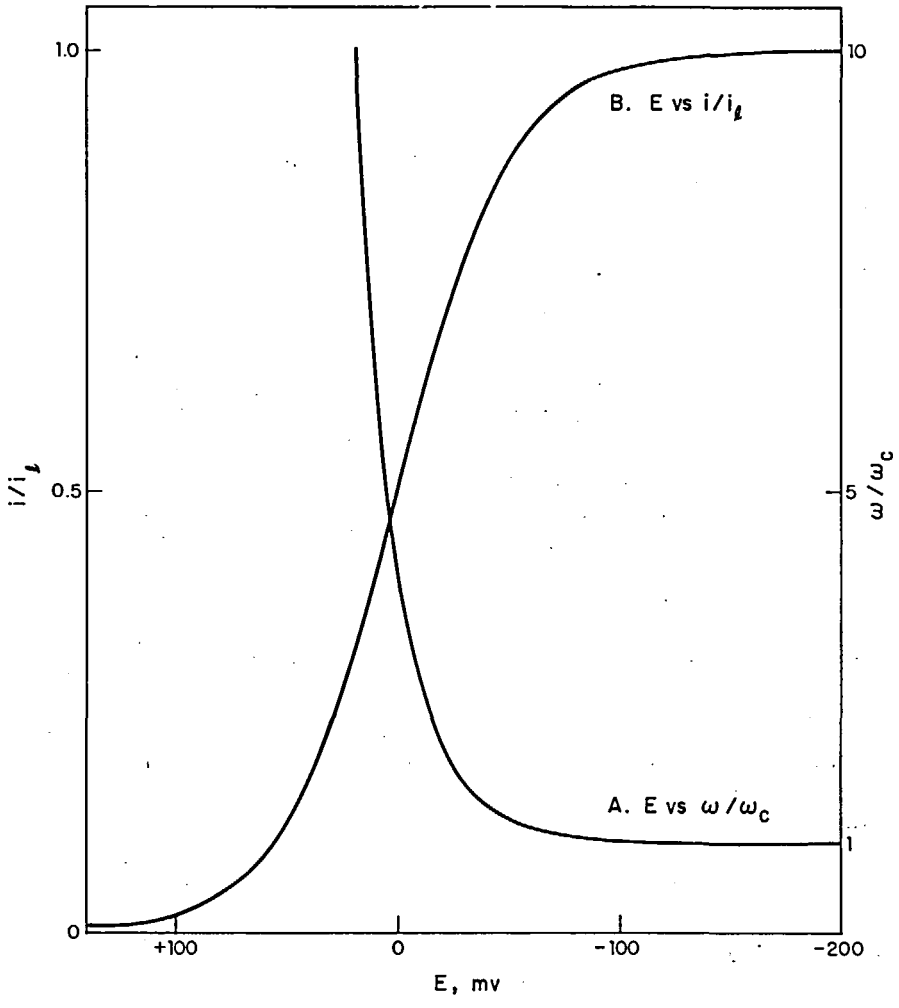

FIGURE 21. Schematic plots of A, E versus ψ at constant disc current and B, disc current versus E at constant rotational velocity.

The differential equations for Y and O include both mass transport and kinetic terms.

$$\frac{\partial C_O(x,t)}{\partial t} = D_O \frac{\partial^2 C_O(x,t)}{\partial x^2} + k_f C_Y(x,t) - k_b C_O(x,t) \quad (86)$$

$$\frac{\partial C_Y(x,t)}{\partial t} = D_Y \frac{\partial^2 C_Y(x,t)}{\partial x^2} - k_f C_Y(x,t) + k_b C_O(x,t) \quad (87)$$

Note that k_f and k_b are first order rate constants and are expressed in molar concentration units rather than as activities. $K = k_f/k_b$ is the equilibrium quotient for the transformation, with concentrations again expressed in molar units rather than as activities.

The initial conditions are that the sum of both O and Y equals the analytical concentration of O, C_O^*, and that the ratio of O to Y is given by K, viz.

$$C_O(x,0)/C_Y(x,0) = K \quad (88)$$

The concentration of O as a function of time was derived by Delahay and Berzins.[66] The transition time is given implicitly by

$$i_o\tau^{1/2} = \frac{\pi^{1/2} nFC^* D^{1/2}}{2} - \frac{\pi^{1/2} i_o}{2K(k_f+k_b)^{1/2}} \operatorname{erf}[(k_f+k_b)^{1/2}\tau^{1/2}] \quad (89)$$

The first term on the right-hand side is the Sand term. The general effect of the preceding chemical reaction is to *decrease* the observed transition time below that predicted by the Sand Equation. For transition times longer than about $4/(k_f + k_b)$ seconds, the error function is nearly unity and $i_o\tau^{1/2}$ decreases linearly with increasing current density.

$$i_o\tau^{1/2} = \frac{\pi^{1/2} nFC^* D^{1/2}}{2} - \frac{\pi^{1/2}}{2K(k_f+k_b)^{1/2}} i_o \quad (90)$$

Of course, at sufficiently low current densities, the electron-transfer process is so slow that the $Y \rightleftarrows O$ interconversion is always approximately at equilibrium and $i_o\tau^{1/2}$ is decreased insignificantly from the Sand value. If one makes the rather optimistic assumption that one can determine transition times accurately down to the millisecond region, the fastest processes that can be investigated by chronopotentiometry correspond[14] to K $(k_f + k_b)^{1/2} \sim 500$ sec$^{-1/2}$. In situations where the equilibrium favors the electroactive species ($K \sim 10$), we are restricted to rate constants slower than about 10^3 sec^{-1}. Since this is rather slow,[117] the principal application of this technique is to cases where the equilibrium favors the electroinactive species.

At very high current densities, the transition time becomes so short that the chemical reaction cannot convert a significant fraction of electroinactive Y to electroactive O. In this limit, $i_o\tau^{1/2}$ is independent of current density but it is proportional to the equilibrium concentration of O, not to the total analytical concentration. Stating this explicitly, one may write

$$\lim_{i_o \to \infty} i_o\tau^{1/2} = \frac{nF(\pi D)^{1/2}}{2} \frac{K C_O^*}{1+K} \quad (91)$$

Note that if one does not have an independent estimate of the diffusion coefficient, and thus of the value of $i_o\tau^{1/2}$ to be expected in the absence of kinetic processes, he might be led to the erroneous conclusion that there was no preceding chemical reaction simply because $i_o\tau^{1/2}$ is constant. Constancy of $i_o\tau^{1/2}$ is a necessary but not sufficient condition whereby one can rule out kinetic complications.

If one were to conduct a current-reversal experiment on a system with a preceding chemical reaction, the ratio of forward to reverse times should be given by Equation 49. This is because the rate of formation of R in the solution is independent of any kinetic process preceding the electron transfer.

However, if one were to reverse the current a second time, the influence of the kinetic prestep would appear.[118]

XV. KINETIC PROCESSES: FOLLOWING REACTIONS

The general scheme we will consider is

$$O + ne = R \underset{k_b}{\overset{k_f}{\rightleftarrows}} Y \quad (92)$$

where the solution is initially free of R and Y. Because Y is not electroactive, and O is not involved in the homogeneous following reaction, the forward transition time will be exactly that predicted by the Sand Equation.

The wave upon current reversal will be shortened, however, because some of the reduced product will be transformed into electroinactive Y. The ratio of forward to reverse times can be used to estimate the rate of the following reaction.[119, 120] The theoretical relationship is

$$2 \text{ erf } (k_f \tau_r)^{\frac{1}{2}} = \text{erf}[k_f(t_f+\tau_r)]^{\frac{1}{2}} \quad (93)$$

where t_f is the forward electrolysis time and τ_r is the transition time upon reversal. The working curve[120] of τ_r/t_f as a function of $t_f k_f$ indicates that the precision of this technique drops off rapidly for processes faster than that where $t_f k_f$ is greater than about three; at this point, the reverse wave is about 1/15 of the forward electrolysis time. The upper limit on rate constants is set by the lower limit on forward electrolysis time. Certainly, $k_f < 10^3$ sec^{-1} is not pessimistic.

If the electron-transfer process is reversible, it is possible to determine the rate of a follow-up reaction by analyzing the shape of the potential-time curve.

The curve is described by Equation 94[14]

$$E = E_{\frac{1}{2}} + \frac{RT}{nF} \ln \frac{\tau^{\frac{1}{2}}-t^{\frac{1}{2}}}{t^{\frac{1}{2}}} - \frac{RT}{nF} \ln \Omega(t) \quad (94)$$

where

$$\Omega(t) = \frac{1}{1+K} + \frac{\pi^{\frac{1}{2}}}{2} \frac{K}{1+K} \frac{\text{erf}[(k_f+k_b)^{\frac{1}{2}}t^{\frac{1}{2}}]}{(k_f+k_b)^{\frac{1}{2}}\, t^{\frac{1}{2}}} \quad (95)$$

As the rate of the homogeneous reaction increases, the E-t curve shifts anodically since the concentration of the reduced form at the electrode surface is decreased. In the limit of a very fast reaction, R and Y may be considered to be in equilibrium. In this limit, Equation 23, describes the shape of the wave but the quarter-wave potential is shifted by RT/nF ln$K$.

Following reactions can also be studied by cyclic chronopotentiometry[118] and thin-layer chronopotentiometry.[4]

XVI. KINETIC PROCESSES: CATALYTIC REACTIONS

$$O + ne = R + Z \xrightarrow{k} O$$

If we assume that substance O is regenerated by a *totally irreversible* first-order or pseudo-first-order process following the electron-transfer reaction, and that $D_O = D_R$, then the concentration of O at the electrode surface is given by[120]

$$C_O(0,t) = C_O^* - \frac{i_o t^{\frac{1}{2}}}{nFD^{\frac{1}{2}}\beta} \text{ erf } \beta \quad (96)$$

where

$$\beta^2 = k\, C_Z^*\, \tau \quad (97)$$

As usual, the transition time is defined by $C_O(0,\tau) = 0$. It is assumed that the concentration of Z at the electrode surface is the same as in the bulk - this is required if the reaction is to be pseudo first order - and this will be true if the "transition time" for the diffusion of Z to the electrode is considerably larger than the transition time for the catalytic reaction. Expressing this mathematically, the restriction on the bulk concentration of Z is

$$\tau_Z^{\frac{1}{2}} >> \tau_C^{\frac{1}{2}}$$

$$\frac{nF\, \pi^{\frac{1}{2}} D^{\frac{1}{2}} C_Z^*}{2\, i_o} >> \frac{nFD^{\frac{1}{2}}\, \beta\, C_O^*}{i_o \text{ erf } \beta}$$

or

$$C_Z^* >> \frac{2\, \beta\, C_O^*}{\pi^{\frac{1}{2}} \text{ erf } \beta} \quad (98)$$

In the limit of a very slow catalytic reaction ($k \to 0$) or high current densities ($\tau \to 0$), the equation for the transition time for the catalytic wave reduces to the Sand Equation. At lower current densities, the transition time becomes quite long, erf $\beta \to 1 - e^{-\beta^2}/\beta\pi^{\frac{1}{2}} + \ldots$, and the equation for the chronopotentiometric constant in the presence of a catalytic reaction becomes[120]

$$\frac{i_o \tau^{\frac{1}{2}}}{C_O^*} = nFD^{\frac{1}{2}}\, \beta; \quad \beta > 2. \quad (99)$$

Rather than being independent of current density, $i_o\tau^{1/2}/C_O^*$ increases with $\tau^{1/2}$ (i.e., with β) at low current densities. Note that this behavior is qualitatively similar to that indicative of a kinetic prestep. However, the high-current-density intercept in the catalytic case will be the Sand term, whereas the high-current-density intercept in the preceding reaction case must be less than the Sand term.

Perhaps the quickest way to distinguish between a preceding chemical reaction and a catalytic reaction is to compare the behavior upon current reversal. The preceding reaction will give rise to a reverse time one third as long as the forward time but the reverse time for a catalytic process will be shortened because some of the product is removed by the catalytic process.

The reverse transition time is related to the forward electrolysis time by exactly the same expression as applies to a following reaction which yields an inactive product, Equation 93.

$$2 \text{ erf } \beta\tau_r^{1/2} = \text{erf}[\beta(t_f+\tau_r)^{1/2}] \qquad (100)$$

The theory has been extended to second-order processes.[123]

Catalytic processes can also be studied by cyclic chronopotentiometry[118] and thin-layer chronopotentiometry.[4]

XVII. KINETIC PROCESSES: THE ECE MECHANISM

The third and final type of following reaction that we will consider occurs when the chemical step produces a species that is immediately further reduced at a diffusion-controlled rate. The reduction of p-nitrophenol and p-nitrosophenol are the archetypes[124] for this mechanism.

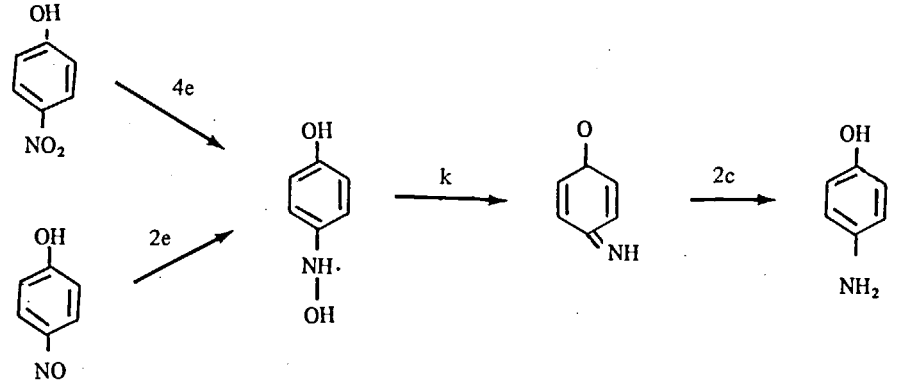

Note that the general scheme is

$$\begin{array}{l} O + ne \rightarrow R \\ \quad\downarrow k \\ \quad O' + n'e \rightarrow R' \end{array}$$

where the chemical process is assumed to be first-order and totally irreversible and where O′ is assumed to be more readily reduced than the starting substrate. This kind of process occurs frequently in organic electrode reactions.

The quantitative behavior of $i_o\tau^{1/2}$ as a function of current density has been derived for this mechanism.[125,126] The qualitative behavior can be predicted for such a system by noting that $i_o\tau^{1/2}$ will be constant and proportional to nC_o^* for transition times short compared to the half life of R, that $i_o\tau^{1/2}$ will increase with increasing transition time in the region where the transition time and the half life of R are comparable, and that $i_o\tau^{1/2}$ will again be constant but now proportional to $(n+n')C_o^*$ for transition times long compared to the half life of R. In the last instance, the chemical reaction is sufficiently fast—relative to the time scale of the experiment—that R is transformed to O′ as rapidly as it is formed.

Note that this behavior is qualitatively quite similar to that predicted for a preceding chemical reaction: at short transition times, $i_o\tau^{1/2}$ is constant and proportional to $C_o^*K/(1+K)$ and, at long transition times, it is again constant but proportional to C_o^*. In fact, at low current densities, it can be shown that[127] $i_o\tau^{1/2}$ for the ECE mechanism should increase linearly with increasing current density. When the long transition time limit of $i_o\tau^{1/2}$ is a nonintegral multiple of the short transition time limit, the mechanism is undoubt-

edly that of a preceding chemical reaction. When the limits are integral multiples of each other, or when the short transition time limit is not accessible, the chronopotentiometric data can probably be interpreted either way and additional information is needed for a decision. The only certain conclusion is that a chemical reaction precedes one of the electron-transfer steps.

The behavior on current reversal will almost certainly distinguish between these two mechanisms. For example, if one is dealing with a preceding chemical reaction, then the product of electron transfer would be stable and one would expect the 1:3 ratio upon reversal. If the process is an ECE mechanism, the reverse wave will be shortened.

The exact behavior of an ECE mechanism on current reversal depends on the thermodynamics and kinetics of the two electron-transfer processes. One of the simplest assumptions, from the point of view of solving the differential equations, is to assume that O continues to be reduced upon current reversal.[118, 126] However, this is unlikely to be the case if the initial electron-transfer process is totally irreversible, in which case the reduction of O′ is likely to cease, or R′ may even be oxidized. Solutions have not been obtained for the latter two possibilities.

We have dealt here, deliberately, with very simple kinetic processes. The real world is often more complex[116, 126-128] and very general approaches to the solution of these kinds of kinetic boundary conditions have been proposed and utilized.[118,129,130]

However, it is my opinion that chronopotentiometry is inherently inferior to fixed potential techniques such as polarography,[16] rotating disc and ring-disc techniques,[131] and chronoamperometry[132] or chronocoulometry[133] for two principal reasons.

In the first place, one must devise a suitable model to correct for the reaction of adsorbed material. This is not to say that one cannot correct for these effects in chronopotentiometry,[54, 126, 134] but rather that it is usually easier to do so with a fixed-potential technique by taking advantage of the different time constants for the charging of the double layer and the reaction of adsorbed material as opposed to the slower diffusion-controlled processes in which we usually are primarily interested.

Secondly, it is very difficult to derive the theoretical chronopotentiometric behavior for two (or more) parallel electron-transfer processes unless there are rather large differences in the potential regions where they occur. For an ECE process, for example, in which the two electron-transfer processes have similar standard potentials and rate constants, it would be necessary to know these standard potentials and the appropriate values of α and of $k_{s,h}$ and to then do a numerical simulation in order to predict the chronopotentiometric behavior. For a controlled-potential experiment, all one need do is adjust the potential so that it is on the diffusion limited plateau of both species.

For these reasons, chronopotentiometry cannot be viewed as a principal tool in the study of homogenous reactions surrounding electron-transfer processes. It does have limited use, however, as a diagnostic tool for the unraveling of simpler, and slower, kinetic mechanisms and to confirm postulated mechanisms for more complex, but still slow, processes.

XVIII. CONCLUSIONS

In rereading this review, I am struck by the recurring negative theme: chronopotentiometry is of limited analytical utility; transition times are badly and perhaps irrevocably lengthened by double-layer charging; quantitative estimation of adsorption isotherms is problematical; double-layer charging limits chronopotentiometry to the measurement of slow electron-transfer processes; and, in the area of homogenous kinetics, chronopotentiometry is a diagnostic tool only. Ev en the occasional mathematical superiority of the technique is denigrated by the increasing use of digital simulation, which is a necessity for the more complex problems anyway.

Furthermore, in surveying the chronopotentiometric literature, I am struck by the fact that new chemical information has only rarely been deduced from chronopotentiometric experiments. The bulk of the literature is concerned with the development of the technique *per se*, rather than its application. This is, to my mind, convincing evidence of the limited applicability and utility of the technique.

Curiously, and this is perhaps because of the academic orientation of most electroanalytical chemists, there are three areas of very great economic importance that have been overlooked

by the devotees of chronopotentiometry: electrowinning, electrorefining, and electroplating of the non ferrous metals. For, to the extent that these processes are controlled at all, they are controlled to approximately constant-current conditions, in other words, quasi-chronopotentiometric conditions. In general, these areas would benefit from an improved understanding of the fundamental electrochemical processes involved. I am not suggesting that chronopotentiometry is necessarily the technique whereby to obtain this information but certainly, once the electrochemical parameters have been defined and evaluated, the wealth of theoretical and practical information about the response of systems under chronopotentiometric conditions will suggest ways to alter these processes to improve both the rate and selectivity of the electrode reactions.

Acknowledgment

The support of the National Science Foundation and the University Computing Center, while the author was at the University of Minnesota, is gratefully acknowledged.

REFERENCES

1. Lingane, J. J., *Electroanalytical Chemistry*, 2nd ed., Interscience, New York, 1958.
2. Kooijman, D. J. and Sluyters, J. H., *J. Electroanal. Chem.*, 13, 152 (1967).
3. Delahay, P., Study of fast electrode processes by relaxation methods, in *Advances in Electrochemistry and Electrochemical Engineering*, Vol. 1, Delahay, P., Ed., Interscience, New York, 1961.
4. Anson, F. C. and Hubbard, A. T., in *Electroanalytical Chemistry*, Vol. 4, Bard, A. J., Ed., Marcel Dekker, Inc., New York, 1970.
5. Lingane, J. J., *Analyst*, 91, 1 (1966).
6. Reinmuth, W. H., *Anal. Chem.*, 33, 485 (1961).
7. Davis, D. G., Applications of chronopotentiometry to problems of analytical chemistry, in *Electroanalytical Chemistry*, Vol. 1, Bard, A. J., Ed., Marcel Dekker, Inc., New York, 1966.
8. Paunovic, M., *J. Electroanal. Chem. Interfacial Electrochem.*, 14, 447 (1967).
9. Adams, R. N., *Electrochemistry at Solid Electrodes*, Marcel Dekker, Inc., New York, 1969.
10. Delahay, P., *New Instrumental Methods in Electrochemistry*, Interscience, New York, 1954, Appendix 2.
11. Delahay, P., *New Instrumental Methods in Electrochemistry*, Interscience, New York, 1954, Chap. 33.
12. Delahay, P., *New Instrumental Methods in Electrochemistry*, Interscience, New York, 1954, Chap. 4.
13. Delahay, P., *J. Amer. Chem. Soc.*, 75, 1430 (1953).
14. Delahay, P., *New Instrumental Methods in Electrochemistry*, Interscience, New York, 1954, Chap. 8.
15. Heyrovsky, J. and Kuta, J., *Principles of Polarography*, Academic Press, New York, 1966, Chap. 16.
16. Heyrovsky, J. and Kuta, J., *Principles of Polarography*, Academic Press, New York, Chap. 17.
17. Feldberg, S. W. and Auerbach, C., *Anal. Chem.*, 36, 505 (1964).
18. Feldberg, S. W., in *Electroanalytical Chemistry*, Vol. 3, Bard, A. J., Ed., Marcel Dekker, Inc., New York, 1969.

19. Reinmuth, W. H., *Anal. Chem.*, 32, 1514 (1960).

20. Bruckenstein, S. and Miller, B., *J. Electrochem. Soc.*, 117, 1040 (1970).

21. Anson, F. C., *Anal. Chem.*, 36, 520 (1964).

22. Osteryoung, R. A., *Anal. Chem.*, 37, 429 (1965).

23. Peters, D. G., Chronopotentiometry, in *Standard Methods of Chemical Analysis*, 6th ed., Part A, Vol. III, Welcher, F. J., Ed., D. Van Nostrand, Princeton, N. J., 1966.

24. See, for example, Symposium on Electroanalytical Instrumentation, *Anal. Chem.*, 38, 1106 (1966).

25. Herman, H. B. and Bard, A. J., *Anal. Chem.*, 37, 590 (1965).

26. English, T. H., *J. Sci. Instrum.*, 3 (1), 69 (1970).

27. Rao, M. L. B., Damjanovic, J., and Bockris, J. O. M., *J. Phys. Chem.*, 67, 2508 (1963).

28. Tatwawadi, S. V. and Bard, A. J., *Anal. Chem.*, 36, 2 (1964).

29. Laitinen, H. A. and Chambers, L. M., *Anal. Chem.*, 36, 5 (1964).

30. Lingane, P. J., *Anal. Chem.*, 39, 485 (1967).

31. Laitinen, H. A., *Anal. Chem.*, 33, 1458 (1961).

32. Lorenz, W., *Z. Elektrochem.*, 59, 730 (1955).

33. Reinmuth, W. H., *Anal. Chem.*, 33, 322 (1961).

34. Broman, R. F. and Murray, R. W., *Anal. Chem.*, 37, 1408 (1965).

35. Lingane, J. J., *J. Electroanal. Chem.*, 1, 379 (1960); 2, 296 (1961).

36. Bard, A. J., *Anal. Chem.*, 35, 340 (1963).

37. Blackburn, T. R. and Lingane, J. J., *J. Electroanal. Chem.*, 5, 216 (1963).

38. Davis, D. G., *Anal Chem.*, 33, 1839 (1961).

39. Evans, D. H. and Lingane, J. J., *J. Electroanal. Chem.*, 8, 173 (1964).

40. Lingane, J. J. and Lingane, P. J., *J. Electroanal. Chem.*, 5, 411 (1963).

41. Morris, M. D. and Lingane, J. J., *J. Electroanal. Chem.*, 8, 85 (1964).

42. Morris, M. D., *J. Electroanal. Chem.*, 8, 350 (1964).

43. Peters, D. G. and Lingane, J. J., *J. Electroanal. Chem.*, 2, 1 (1964).

44. Peters, D. G. and Shults, W. D., *J. Electroanal. Chem.*, 8, 200 (1964).

45. Anson, F. C., *Anal. Chem.*, 33, 1123 (1961).

46. Murray, R. W., *J. Electroanal. Chem.*, 7, 242 (1964).

47. Murray, R. W. and Gross, D. J. *Anal. Chem.*, 38, 392 (1966).

48. Murray, R. W. and Gross, D. J., *Anal. Chem.*, 38, 405 (1966).

49. Munson, R. A., *J. Phys. Chem.*, 66, 727 (1962); *J. Electroanal. Chem.*, 5, 292 (1963).

50. Hamilton, W. C., *Statistics in Physical Science*, Ronald Press, New York, 1964, Chap. 2.

51. Sturrock, P. E., Privett, G., and Tarpley, A. R., *J. Electroanal. Chem. Interfacial Electrochem.*, 14, 303 (1967).

52. Osteryoung, R. A. and Christie, J. H., *Anal. Chem.*, 38, 1620 (1966).

53. Osteryoung, R. A. and Christie, J. H., *J. Phys. Chem.*, 71, 1348 (1967).

54. Noonan, F. J., Ph.D. Thesis, Columbia University, 1967, available from University Microfilms, Inc., Ann Arbor, Mich., #67-9360.

55. Shults, W. D., Haga, F. E., Mueller, T. R., and Jones, H. C., *Anal. Chem.*, 37, 1415 (1965).

56. Anson, F. C., *Anal. Chem.*, 38, 54 (1966).

57. Rodgers, R. S. and Meites, L., *J. Electroanal. Chem. Interfacial Electrochem.*, 16, 1 (1968).

58. DeVries, W. T., *J. Electroanal. Chem. Interfacial Electrochem.*, 17, 31 (1968); 18, 469 (1968); 19, 41 (1968).

59. Olmstead, M. L. and Nicholson, R. S., *J. Phys. Chem.*, 72, 1650 (1968).

60. Olmstead, M. L. and Nicholson, R. S., *Anal. Chem.*, 42, 796 (1970).

61. Reilley, C. N., Everett, G. W., and Johns, R. H., *Anal. Chem.*, 27, 483 (1955).

62. Voorhies, J. D. and Furman, N. H., *Anal. Chem.*, 30, 1656 (1958).

63. Iwamoto, R. T., *Anal. Chem.*, 31, 1062 (1959).

64. Peters, D. G. and Burden, S. L., *Anal. Chem.*, 38, 530 (1966).

65. Shults, W. D. and Mueller, T. R., *J. Electroanal. Chem.*, 12, 354 (1966).

66. Delahay, P. and Berzins, T., *J. Amer. Chem. Soc.*, 75, 2486 (1953).

67. Kuwana, T., unpublished, referenced by Russell and Peterson[70] and Adams,[9] but see also Delahay and Mamantov.[68]

68. Delahay, P. and Mamantov, G., *Anal. Chem.*, 27, 478 (1955).

69. Laity, R. W. and McIntyre, J. D. E., *J. Amer. Chem. Soc.*, 87, 3806 (1965).

70. Russel, C. D. and Peterson, J. M., *J. Electroanal. Chem.*, 5, 467 (1968).

71. DeVries, W. T., *J. Electroanal. Chem. Interfacial Electrochem.*, 19, 55 (1968).

72. Hurwitz, H. and Gierst, L., *J. Electroanal. Chem.*, 2, 128 (1961).

73. Bard, A. J., *Anal. Chem.*, 33, 11 (1961).

74. Evans, D. H. and Price, J. E., *J. Electroanal. Chem.*, 5, 77 (1963).

75. Dornfeld, D. I. and Evans, D. H., *J. Electroanal. Chem. Interfacial Electrochem.*, 20, 341 (1969).

76. Lingane, J. J., *J. Electroanal. Chem.*, 2, 46 (1961).

77. Lingane, P. J., *Anal. Chem.*, 36, 1723 (1964).

78. Soos, Z. G. and Lingane, P. J., *J. Phys. Chem.*, 68, 2321 (1964).

79. Mamantov, G. and Delahay, P., *J. Amer. Chem. Soc.*, 76, 5323 (1954).

80. Jones, J. G., Ph.D. thesis, California Institute of Technology, 1967.

81. Turnham, D. S., *J. Electroanal. Chem.*, 9, 440 (1965).

82. Murray, R. W. and Gross, D. J., *J. Electroanal. Chem. Interfacial Electrochem.*, 13, 132 (1967).

83. Kuempel, J. R. and Schaap, W. B., *J. Electroànal. Chem.*, 12, 77 (1966).

84. Sheaffer, J. C. and Peters, D. G., *Anal. Chem.*, 44, 430 (1970).

85. Berzins, T. and Delahay, P., *J. Amer. Chem. Soc.*, 75, 4205 (1953).

86. Evans, D. H., *J. Electroanal. Chem.*, 9, 267 (1965).

87. Anaon, F. C. and Lingane, J. J., *J. Amer. Chem. Soc.*, 79, 1015 (1957).

88. Herman, H. B., Tatwawadi, S.V., and Bard, A. J., *Anal. Chem.*, 35, 2211 (1963).

89. Macero, D. J. and Anderson, L. B., *J. Electroanal. Chem.*, 6, 221 (1963).

90. Anderson, L. B. and Macero, D. J., *Anal. Chem.*, 37, 322 (1965).

91. Beyerlein, F. H. and Nicholson, R. S., *Anal. Chem.*, 40, 286 (1968).

92. Keis, H. L., *J. Electroanal. Chem.*, 4, 156 (1962).

93. Morris, M. D. and Lingane, J. J., *J. Electroanal. Chem.*, 6, 300 (1963).

94. Morris, M. D., *J. Electroanal. Chem.*, 8, 1 (1964).

95. Anson, F. C., *J. Phys. Chem.*, 71, 3607 (1967).

96. Parsons, R., *Proc. Int. Cong. Surface Activity*, 2nd ed., London, 1957, 3, 38 (1957).

97. Parsons, R., *Proc. Int. Cong. Surface Activity*, 2nd, ed., London, 1957, 3, 38 (1957), Figure 1.

98. Grahame, D. C., *Chem. Revs.*, 41, 441 (1947).

99. Lingane, P. J., Ph.D. thesis, California Institute of Technology, 1966.

100. Broadhead, J. and Hills, G. J., *J. Electroanal. Chem. Interfacial Electrochem.*, 13, 354 (1957).

101. Lingane, P. J., unpublished results, 1970.

102. Joshi, K. M. and Parsons, R., *Electrochem. Acta.*, 4, 129 (1961).

103. Snead, W. K. and Remick, A. E., *J. Amer. Chem. Soc.*, 79, 6121 (1959).

104. Kowalski, T. A. and Lingane, P. J., submitted for publication.

105. Deming, W. E., *The Statistical Adjustment of Data*, Dover, New York, 1964.

106. Hamilton, W. C., *Statistics in Physical Science*, Ronald Press, New York, 1964.

107. Lingane, P. J. and Hugus, Z. Z., Jr., *Inorg. Chem.*, 9, 757 (1970).

108. Moore, R. H. and Ziegler, R. K., LA-2367, (1959), U.S. Government Printing Office, Washington, D.C., Section 2.3.

109. Kowalski, T. A., M.S. thesis, University of Minnesota, Dec. 1970.

110. For example, Brown, E. R., Smith, D. E., and Brown, G. L., *Anal. Chem.*, 40, 1410 (1968).

111. Buck, R. P. and Keller, H. E., *Anal. Chem.*, 35, 400 (1963).

112. Hsueh, L. and Newman, J., *Electrochimica Acta.*, 12, 429 (1967).

113. Miller, B. and Bruckenstein, S., *J. Electrochem. Soc.*, 117, 1032 (1970).

114. Herman, H. B. and Blount, H. N., *J. Electroanal. Chem. Interfacial Electrochem.*, 25, 165 (1970).

115. Murray, R. W. and Reilley, C. N., *J. Electroanal. Chem.*, 3, 64 (1962).

116. Herman, H. B., in *Electroanalytical Chemistry*, Bard, A. J., Ed., Marcel Dekker, Inc., New York, 1971, in press.

117. Cladin, E. F., *Fast Reactions in Solution*, Blackwell, Oxford, 1964.

118. Herman, H. B. and Bard, A. J., *J. Electrochem. Soc.*, 115, 1028 (1968).

119. Dracka, O., *Collect. Czech. Chem. Commun.*, 25, 338 (1960).

120. Testa, A. C. and Reinmuth, W. H., *Anal. Chem.*, 32, 1512 (1960).

121. Delahay, P., Mattax, C. C., and Beizins, T., *J. Amer. Chem. Soc.*, 76, 5319 (1954).

122. Furlani, C. and Morpurgo, G., *J. Electroanal. Chem.*, 1, 351 (1959).

123. Fischer, O., Dracka, O., and Fischerova, E., *Collect. Czech. Chem. Commun.*, 26, 1505 (1961).

124. Blount, H. N. and Herman, H. B., *J. Phys, Chem.*, 72, 3006 (1968) and references therein.

125. Testa, A. C. and Reinmuth, W. H., *J. Amer. Chem. Soc.*, 83, 783 (1961).

126. Herman, H. B. and Bard, A. J., *J. Phys. Chem.*, 70, 396 (1966).

127. Testa, A. C. and Reinmuth, W. H., *Anal. Chem.*, 33, 1320 (1961).

128. Hawley, M. D. and Feldberg, S. W., *J. Phys. Chem.*, 70, 3459 (1966).

129. Hung, H. C., Delmastro, J. R., and Smith, D. E., *J. Electroanal. Chem.*, 7, 1 (1964).

130. Ashley, J. W. and Reilley, C. N., *J. Electroanal. Chem.*, 7, 253 (1964).

131. Prater, K. B. and Bard, A. J., *J. Electrochem. Soc.*, 117, 335 (1970).

132. Schwartz, W. M. and Shain, I., *J. Phys. Chem.*, 69, 30 (1965).

133. Christie, J. H., *J. Electroanal. Chem. Interfacial Electrochem.*, 13, 79 (1967).

134. Evans, D. H., *Anal. Chem.*, 36, 2027 (1964).

135. Lingane, P. J., *Inorg. Chem.*, 9, 1152 (1970).

136. Burden, S. L., Ph.D. thesis, University of Indiana, 1966.

137. Peters, D. G., Ph.D. thesis, Harvard University, 1962.